CHAPTER 7

ASSESSMENT OF RIVER CHANNEL CHANGE

CHAPTER 7 ASSESSMENT OF RIVER CHANNEL CHANGE

7.1 Channel Changes in the Upper Reach of Ratu River

(1) Spectral Characteristics of Deposited Materials

Identification of the channel changes of the upper reach of Ratu river was attempted using satellite data. The river bed appears very bright on aerial photographs, and on the conventional photographs indicating very high reflectance in the visible spectral region of the Electromagnetic spectrum. Further, some form of gradation different was observed in the old deposits. It was attempted to observe these characteristic properties on the radiance values observed by the sensors to establish the best suitable spectral band or the combination of bands for delineating accumulation of deposition, and assessing the change of deposition.

With reference to the aerial and other conventional photographs reference areas were established and corresponding digital counts for water, forest, crop lands and river sediments covering most of the study area were extracted. Statistical parameters for representative sample areas were calculated and analyzed for spectral characteristics for differentiation of these cover classes and to establish the spectral characteristics of deposited materials. The spectral response patterns of the cover classes are depicted graphically in Figure 7.1, 7.2, 7.3 and 7.4 for 1973, 1977, 1993 and 1995 datasets, respectively. Comparatively very high reflectance was observed for riverbed, followed by crop lands and forest. It is said that the bare lands are highly reflective as there is no energy absorption capacity unless the surface is wet. Further, when the materials are very fine and sandy where the water retention power is small, the reflectance tend to be very high compared to other earth features. This is clearly visible in this area as field survey reported that the very fine sandy particles are found in the lower part of the river and there is no visible water flow during the dry period. The riverbed materials in the upper
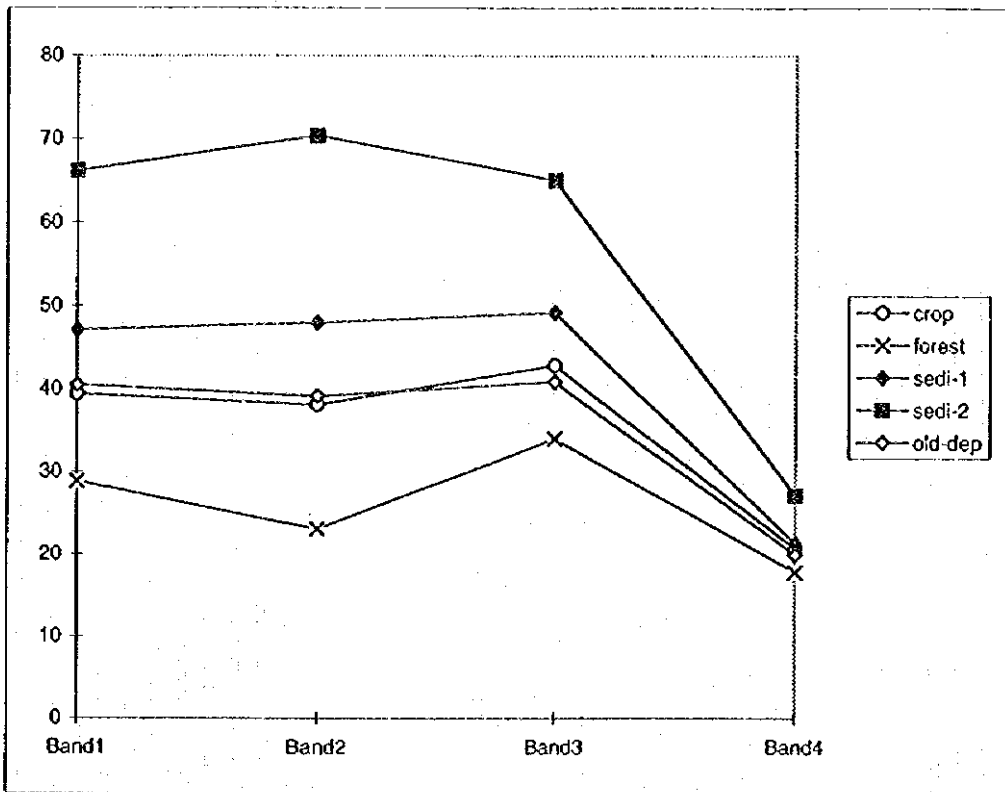
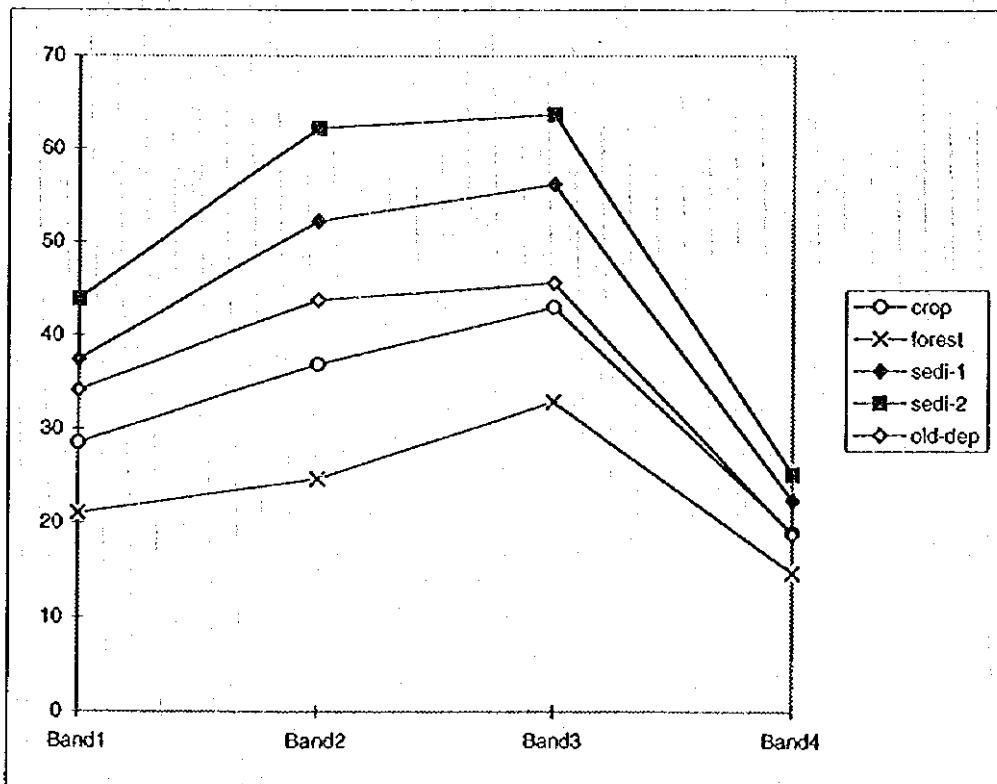Figure 7.1   1973 Landsat MSS spectral response patterns

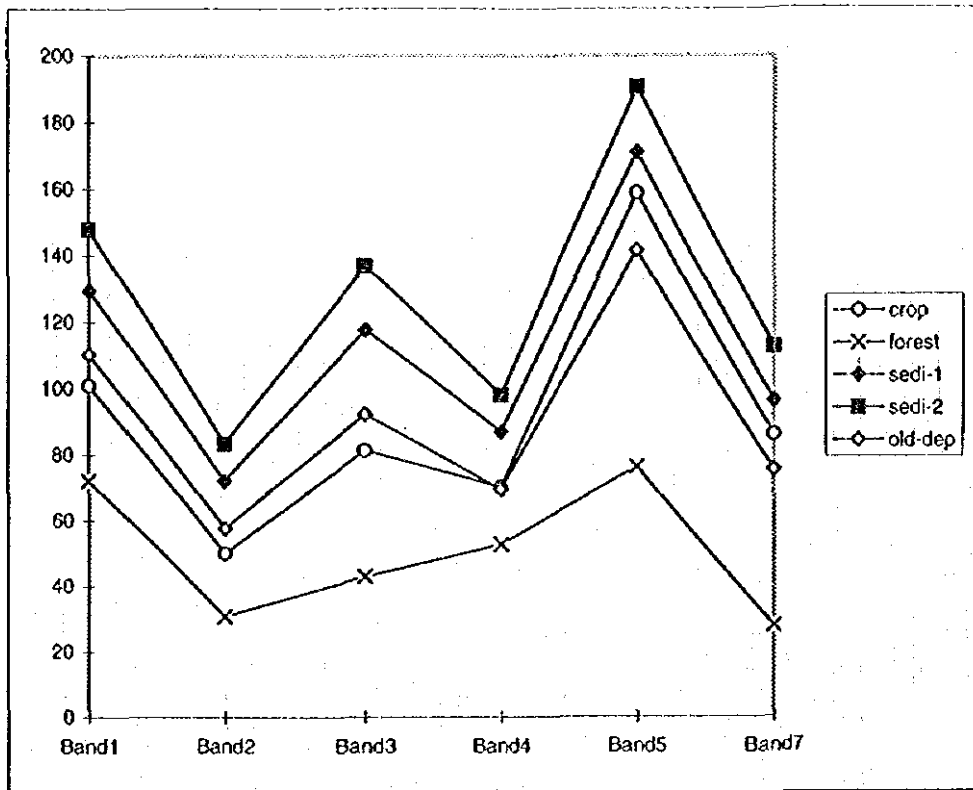Figure 7.2   1977 Landsat MSS spectral response patterns

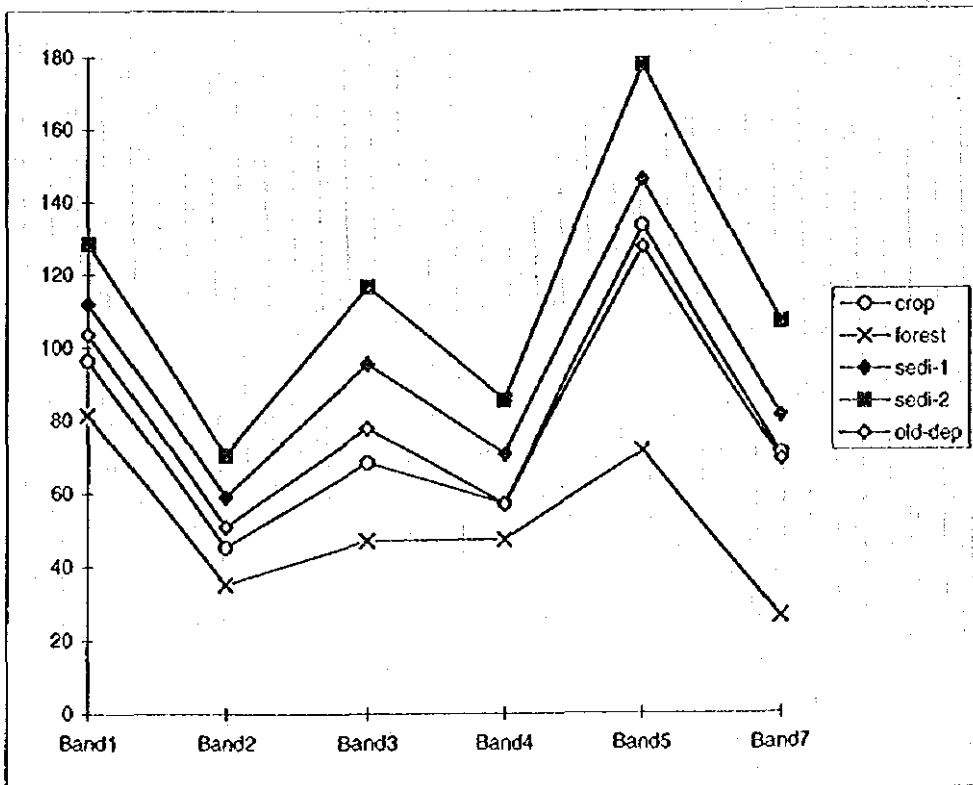Figure 7.3   1993 Landsat TM spectral response patterns

Figure 7.4   1995 Landsat TM spectral response patterns

stream showed less reflectance than the lower area, *sedi-1* for upper reach and *sedi-2* for floodplain in the figures. These difference could be due to particle size or composition, presence of moisture or the trace of the river flow. This was not further investigate at the present study due to lack of survey data for verification. Finally, it could be said that any of the TM spectral band, specially, band 1, band 3, band 5 and band 7 are very much suitable for classification of river bed degradation and aggradation and there is no necessity to establish any other derived index. For MSS, the best band would be band 4, band 5 or band 6. Band 7 may not be very much suitable due to its narrow dynamic range.
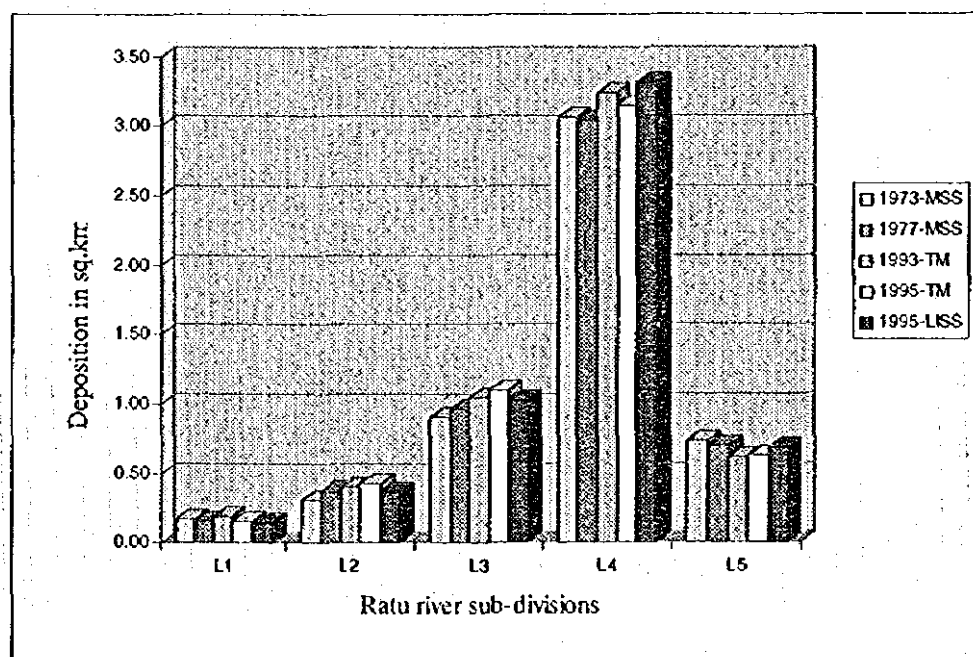

Figure 7.5 Channel change in the Ratu watershed

(2) Estimation of Channel Changes

Using the statistical parameters, means and standard deviations, four days satellite datasets were classified into deposited and non-deposited areas. The extents of the classification are graphically shown in Figure 7.5. Extents of riverbed area is calculated for the sub-divisions of main stream (L1 to L5), and

for other sub-watersheds given in the Figure 7.6, are shown in Table 7.1. These changes in the main stream in the upper watershed for the four days satellite data is shown in Figure 7.7. The estimation of the LISS dataset that that was acquired for comparison with TM data also shown in the figure. There was no general pattern or a trend in the change of riverbed within the upper reach as the changes in the sub-sections did not show continuous increase or decrease. Table 7.2 and Figure 7.8 was constructed for enhance the patter of changes within sub-sections. Cumulative total riverbed area is given in Table 7.2, and the of change of area with respect to that of 1973 is depicted in figure 7.8. It is clear in the figure that the change of the riverbed area is inconsistent, but the total extent from 1973 to 1995 has been increased from 5.2 sq. km. to 5.44sq. km. Riverbed area in 1993 is higher than that of 73 except for the main-5, and considerable expansion was observed in main-2 during the 1973-79 time span.
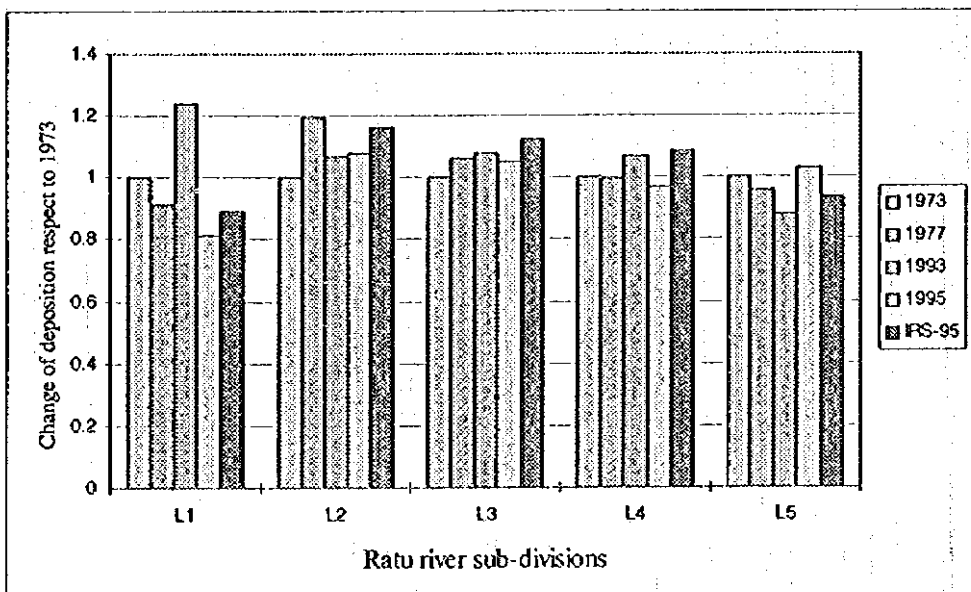

Figure 7.8 Riverbed extent and its change in the upper watershed respect to 1973 bed area
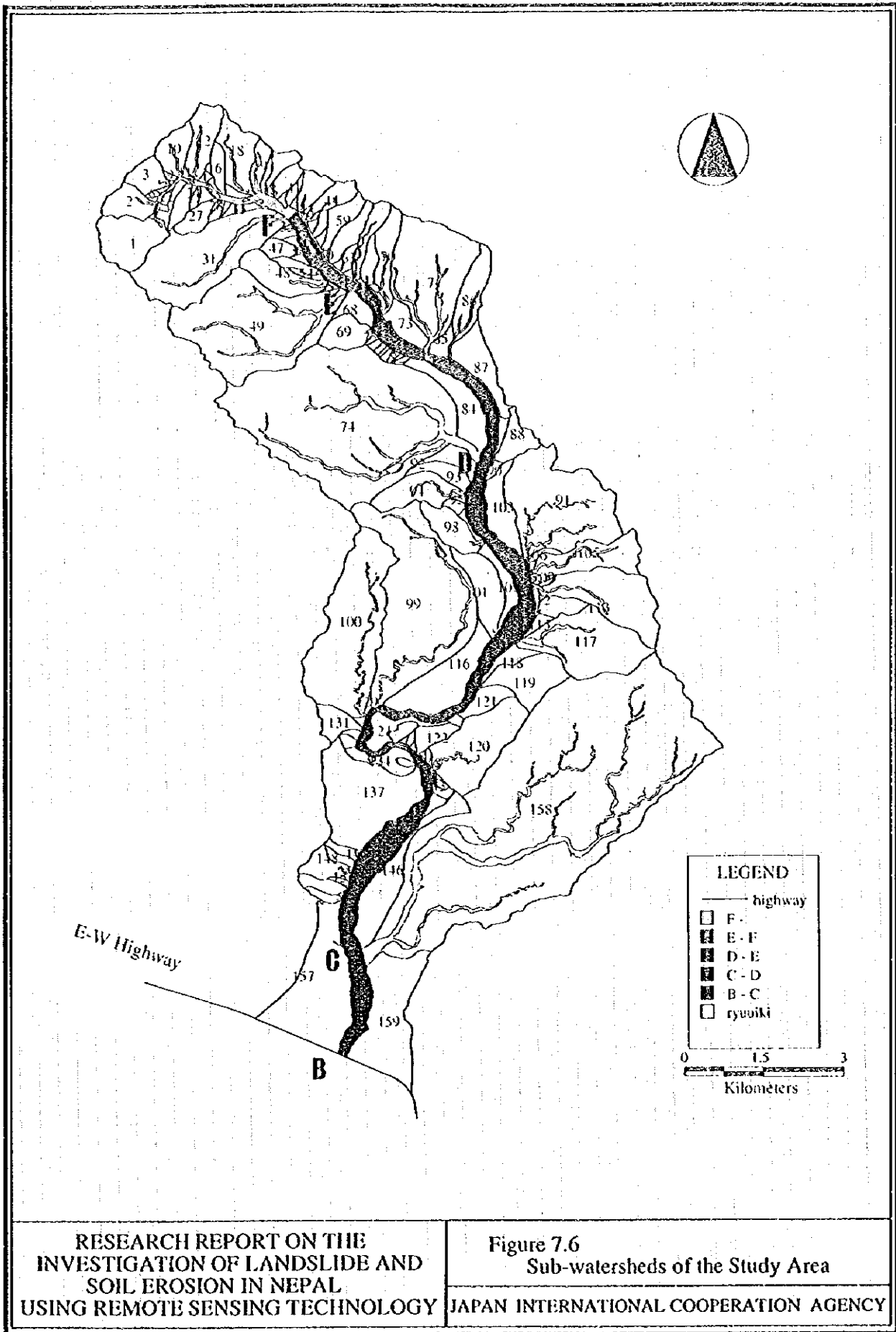
LEGEND

———— highway
☐ F ·
▨ E · F
▨ D · E
▨ C · D
▨ B · C
☐ ryuuiki

0   1.5   3
Kilometers

E-W Highway

RESEARCH REPORT ON THE INVESTIGATION OF LANDSLIDE AND SOIL EROSION IN NEPAL USING REMOTE SENSING TECHNOLOGY	Figure 7.6 Sub-watersheds of the Study Area
	JAPAN INTERNATIONAL COOPERATION AGENCY
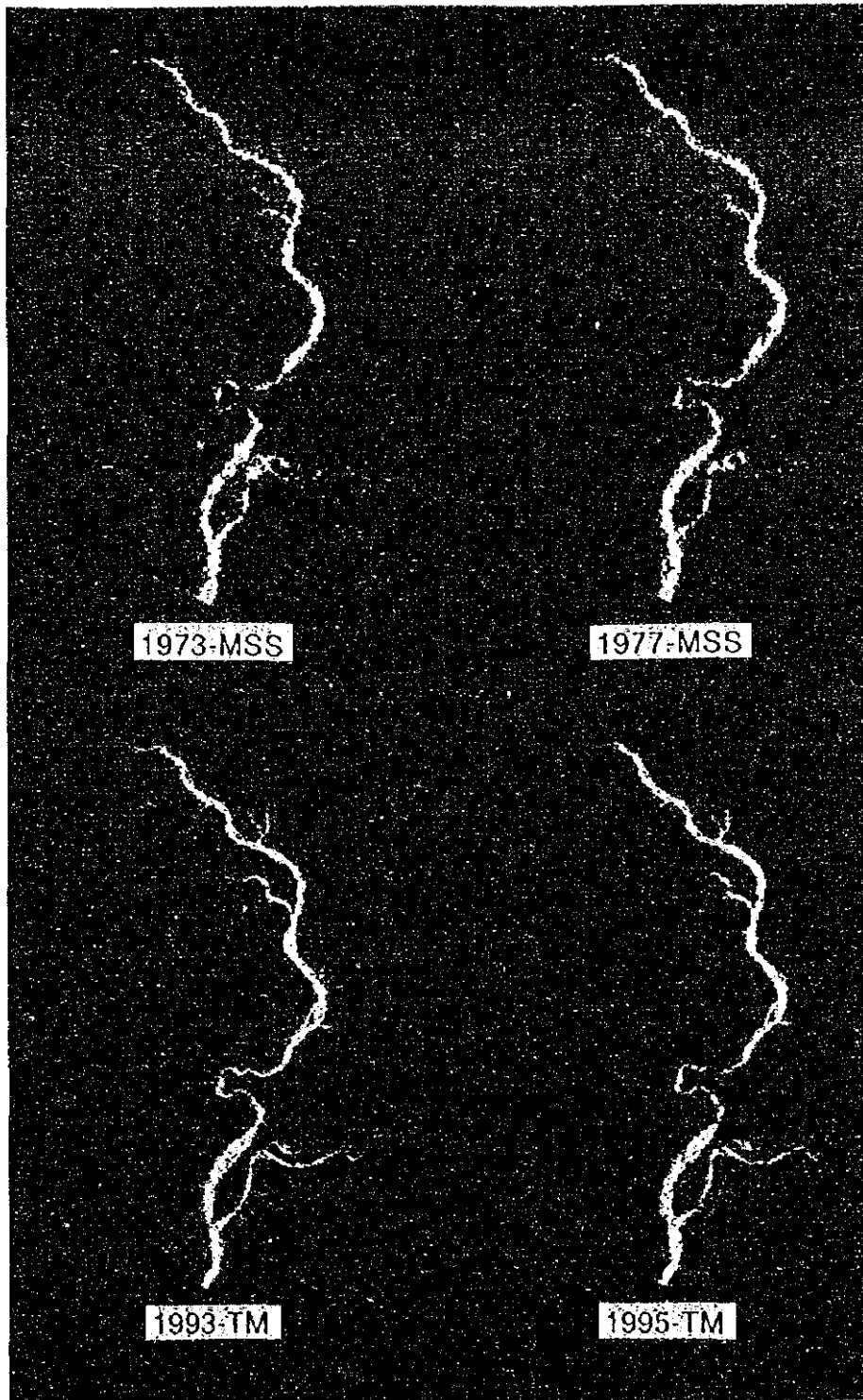
1973-MSS

1977-MSS

1993-TM

1995-TM

LEGEND

Deposition

0   4.0   8.0 km

1 : 200,000

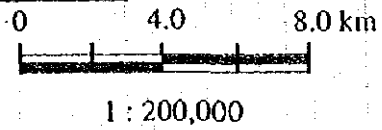| RESEARCH REPORT ON THE INVESTIGATION OF LANDSLIDE AND SOIL EROSION IN NEPAL USING REMOTE SENSING TECHNOLOGY	Figure 7.7 Deposition changes in upper watershed estimated using satellite data
	JAPAN INTERNATIONAL COOPERATION AGENCY

Table 7.1 Sediment depsoition in the main stream and tributaries using satellite data

	1973-MSS	1977-MSS	1993-TM	1995-TM	1995-LISS
L1	0.1692	0.1548	0.1917	0.1557	0.1503
L2	0.3132	0.3744	0.3996	0.4311	0.3636
L3	0.9108	0.9684	1.0431	1.0944	1.0215
L4	3.0564	3.0384	3.2400	3.1383	3.3120
main-5 - to highway	0.7272	0.6948	0.6111	0.6273	0.6813
watershed - 70	0.0000	0.0000	0.0117	0.0171	0.0036
watershed - 71	0.0036	0.0144	0.1440	0.1602	0.0738
watershed - 63	0.0000	0.0000	0.0000	0.0009	0.0000
watershed - 48	0.0000	0.0000	0.0090	0.0045	0.0063
watershed - 49	0.0360	0.0468	0.0441	0.0261	0.0306
watershed - 86	0.0000	0.0036	0.0126	0.0162	0.0027
watershed - 91	0.0000	0.0000	0.0279	0.0108	0.0090
watershed - 105	0.0000	0.0000	0.0135	0.0054	0.0054
watershed - 100	0.0000	0.0000	0.0036	0.0027	0.0009
watershed - 113	0.0000	0.0072	0.0126	0.0072	0.0045
watershed - 117	0.0000	0.0072	0.0522	0.0432	0.0324
watershed - 158	0.8424	0.6156	1.0728	0.9081	0.9090
watershed - 122	0.0000	0.0000	0.0108	0.0027	0.0018
watershed - 31	0.0036	0.0072	0.0108	0.0027	0.0036
watershed - 74	0.1188	0.1800	0.3267	0.2727	0.1611
watershed - 94	0.0000	0.0000	0.0000	0.0018	0.0000
watershed - 101	0.0000	0.0000	0.0243	0.0018	0.0000

Table 7.2 Cumulative area of the riverbed of the main stream

	1973	1977	1993	1995
L1	0.1692	0.1548	0.1917	0.1557
L2	0.4824	0.5292	0.5913	0.5868
L3	1.3932	1.4976	1.6344	1.6812
L4	4.4496	4.5360	4.8744	4.8195
L5	5.1768	5.2308	5.4855	5.4468

The riverbed changes can be due to different patterns of accumulation and erosion of the sub-division of the river, transport capacity of the storm water during flood events, and the characteristics of sub-watersheds that supply the eroded materials. The assumption that was made in chapter 6 describing the Ratu upper region as a transfer zone is further validate as the eroding and depositing nature was observed in the upper stream.

Table 7.3 illustrate the change of the area of deposit within the time intervals of the acquired satellite datasets. Except for the period 1993 to 95, which is relatively a small time span the area of riverbed has been increasing.

Table 7.3 Estimation of riverbed change Index of Ratu river

	1973-77 (sq. km)	1977-93 (sq. km)	1993-95 (sq. km)	1973-95 (sq. km)
Change of area	0.054	0.255	-0.032	0.277
Time interval	4	16	2	22
Deposition Index/year	0.014	0.016	-0.016	0.013

Attempt was made to establish an index that could be used as a guideline for the rate of river expansion in the Ratu watershed using the satellite data estimates for the period of 22 years from 1973 to 95. Change for each time lap was calculated and the annual rate of change was obtained, Table 7.3. The larger time intervals, 73 to 79 and 77 to 93 showed similar rate of increase of the sediment deposition. In contrast to that, the 1993 to 95 showed decrease of

deposition. The flood event that taken place in 1993 might have washed out or eroded the riverbed leaving less deposited materials than in 1993. Also, for the whole time interval, from 1973 to 95 the calculated riverbed change index was almost similar to that of others except for the period 93 to 95. Therefore, a value of about 0.014 sq. km per year could be a reliable deposition index for the Ratu watershed considering 20 year time interval including flood events.

## 7.2 Floodplain Changes and Sedimentation in the Downstream of Ratu River

As for the upper reach of the river, the sediment deposition and its change was estimated for the Ratu floodplain using acquired satellite data. The spectral patterns described in the previous section was used for the classification. The spectral patterns of the category referred to as *sedi-2* in the Figure 7.1 to 7.4 were the representation of sediment in the floodplain of the watershed, specifically on the riverbed. Relatively high spectral response patterns of this category represent the nature of the deposit material, which is fine sand and relatively dry when compared to the same in the upper reach.

The classified Landsat TM data of 1993 for the whole river system is shown in Figure 7.9. Further, the extents of the sediment deposition in the floodplain for the four dates datasets and for the LISS dataset is listed in Table 7.4

Table 7.4 Floodplain deposition of sediment and its change

73-MSS	77-MSS	93-TM	95-TM	95-LISS
sq. km	sq. km	sq. km	sq. km	sq. km
9.1656	11.5956	9.1512	9.6012	10.0685

The figures given in the table represents the whole sediment deposited area below the Highway along the downstream until the satellite sensor can discern the sediment from its surrounding. Further, the given extents exclude the old riverbed deposits that was differentiable by respective sensors of the four dates data. The old deposits spectral response patterns can be distinguishable from

LEGEND

☐ Deposited area

------ Watershed

0   3.5   7.0 km
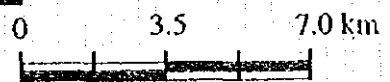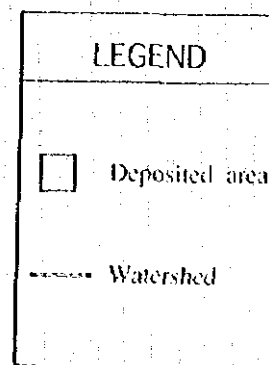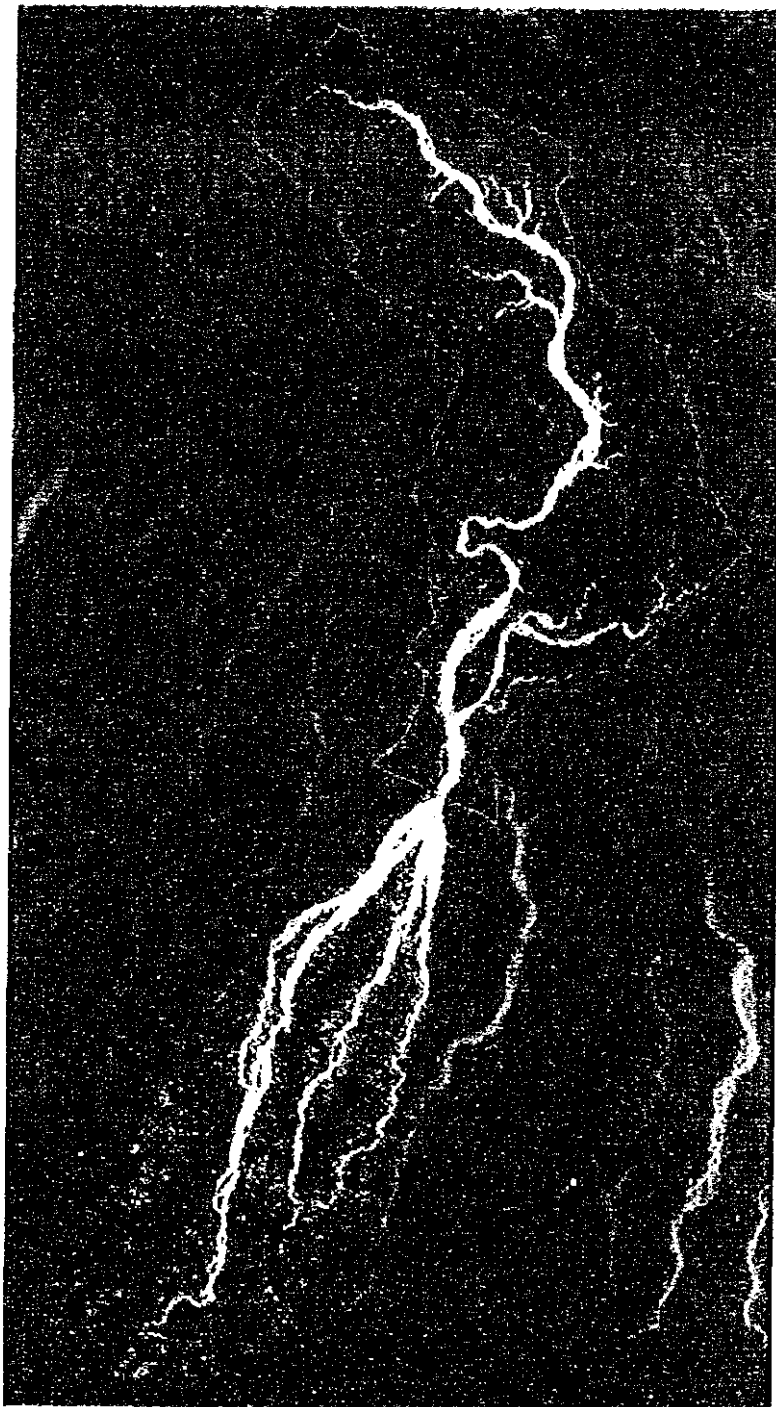
1 : 175,000

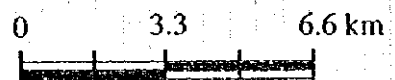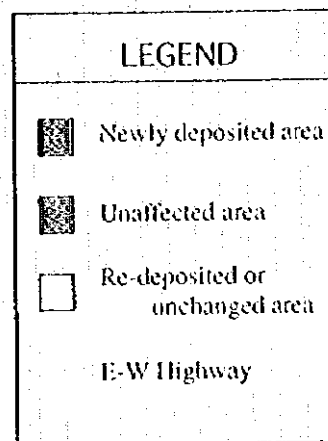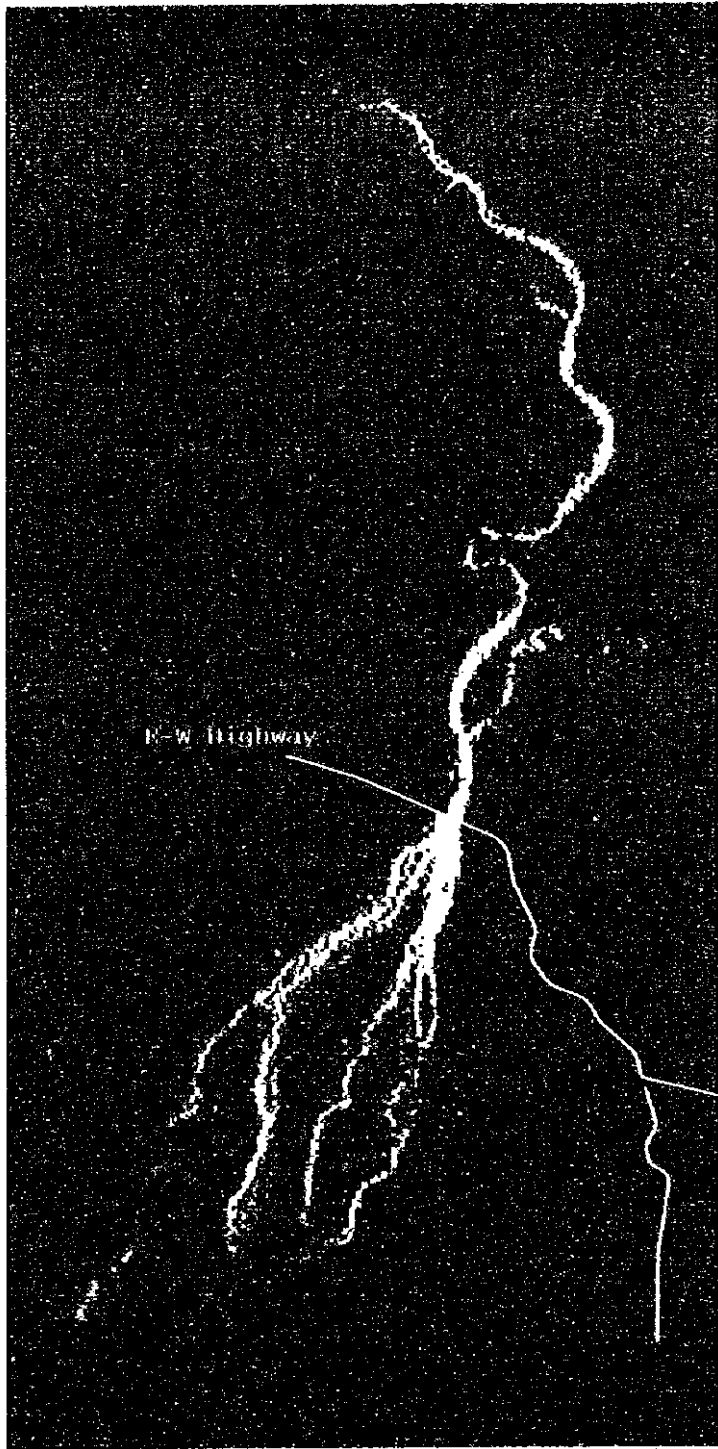| RESEARCH REPORT ON THE INVESTIGATION OF LANDSLIDE AND SOIL EROSION IN NEPAL USING REMOTE SENSING TECHNOLOGY	Figure 7.9 Deposited area estimated for Ratu river using 1993 March TM data
	JAPAN INTERNATIONAL COOPERATION AGENCY

recent deposits, Figure 7.1 to 7.4. Relative decrease of response when compared to new deposits could be due to change of color of the deposit material with time, or sparsely grown grass over the deposited material. The estimations are the observed area of deposit at the time of satellite pass without distinguishing the differences in the deposited areas among the datasets. Table 7.4 clearly shows the area of the deposit is increasing gradually, except for drastic increase in the time span between 1973 to 77. The classification accuracy of LISS shows that LISS sensor data can be used in lieu of Landsat TM data.

Image integration technique was used to further enhance the pattern of deposition and spatial variability of river channel change. A set of three images were produced by integrating two dataset at a time defining three different pattern of changes. Figure 7.10, 7.11 and 7.12 show the *changed*, *unchanged* or *re-deposited/ unaffected* areas during the time intervals 1973-77, 1977-93, and 1993-95 respectively. Light blue represents the newly deposited areas, orange for unaffected areas and re-deposited or unchanged areas are depicted in white.

A considerable increase during the period 73 to 79 was clearly visible in the Figure 7.10, specially in the most westward stream channel. Presence of white deposits in this channel indicates that it was subjected to deposition prior to 1973, but the excessive flow during the 73-77 time period is comparatively very much larger than that has been occurring prior to 1973 This change could be due to alteration of riverbed topography. Deposition in the low flow period might have formed a natural levee in the riverbed below the Highway limiting the flow towards eastern side might be the reason for this change. Decrease in the sediment transportation in the lower portion of the most eastern channel would further support this assumption.

Figure 7.11 shows the difference of the 16 year period from 1977 to 1993. Large area of orange color account for loss of activity in some channels, and the emerge of blue color river patterns show newly formed deposited areas. beneath the Highway the channel bed width has been decreased due to
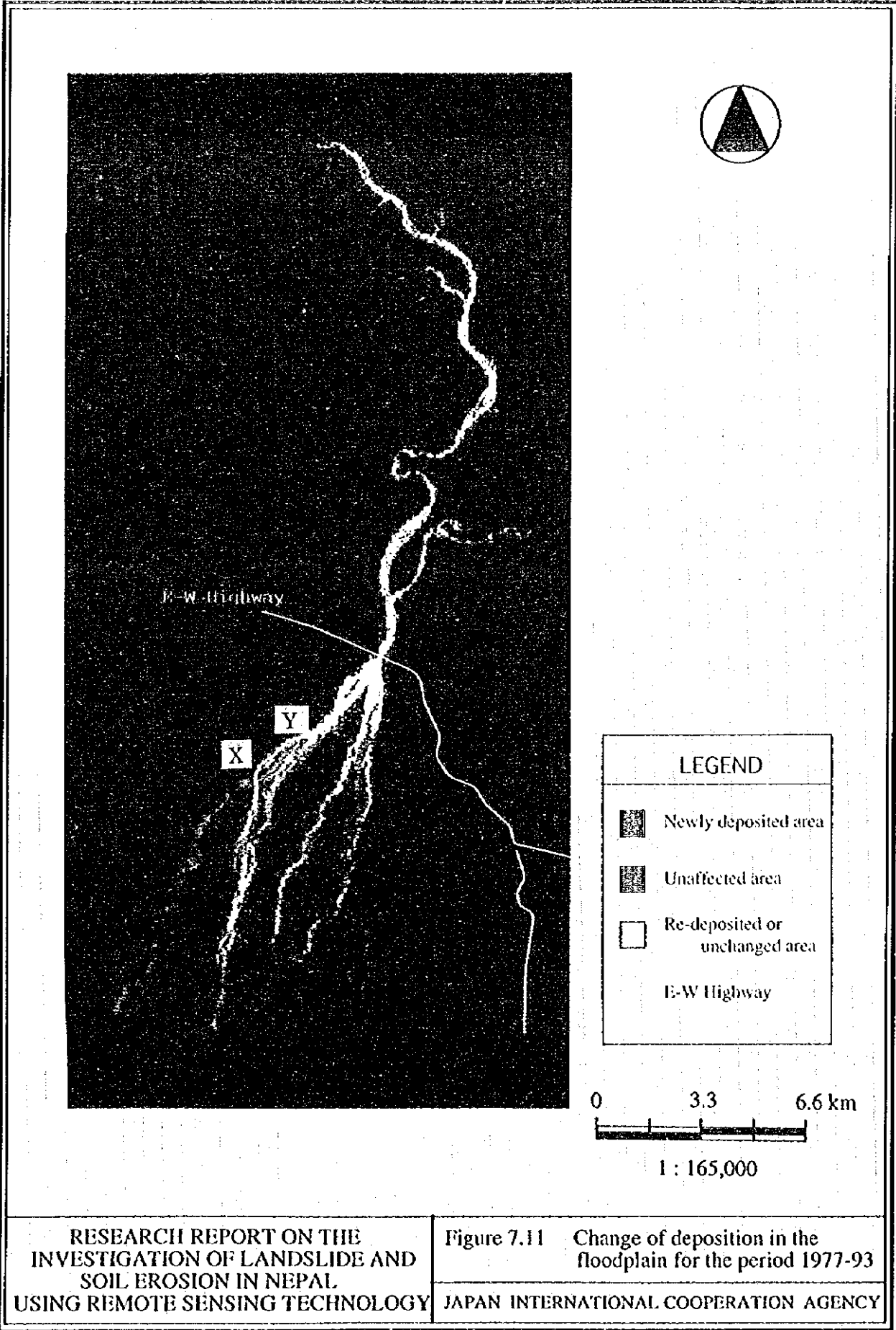
LEGEND

Newly deposited area

Unaffected area

Re-deposited or
unchanged area

E-W Highway

0   3.3   6.6 km

1 : 165,000

RESEARCH REPORT ON THE INVESTIGATION OF LANDSLIDE AND SOIL EROSION IN NEPAL USING REMOTE SENSING TECHNOLOGY	Figure 7.10 Change of deposition in the floodplain for the period 1973-77
	JAPAN INTERNATIONAL COOPERATION AGENCY

Figure 7.11 Change of deposition in the floodplain for the period 1977-93

LEGEND

Newly deposited area

Unaffected area

Re-deposited or unchanged area

E-W Highway

0   3.3   6.6 km

1 : 165,000

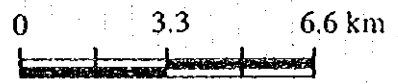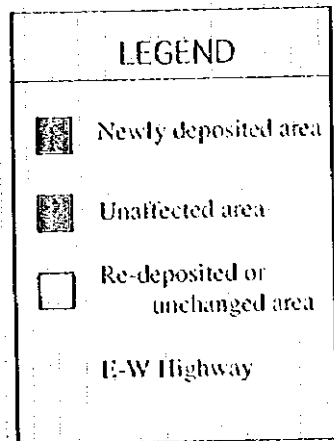| RESEARCH REPORT ON THE INVESTIGATION OF LANDSLIDE AND SOIL EROSION IN NEPAL USING REMOTE SENSING TECHNOLOGY	Figure 7.11 Change of deposition in the floodplain for the period 1977-93
	JAPAN INTERNATIONAL COOPERATION AGENCY

E-W Highway

LEGEND

Newly deposited area

Unaffected area

Re-deposited or
unchanged area

E-W Highway

0   3.3   6.6 km

1 : 165,000

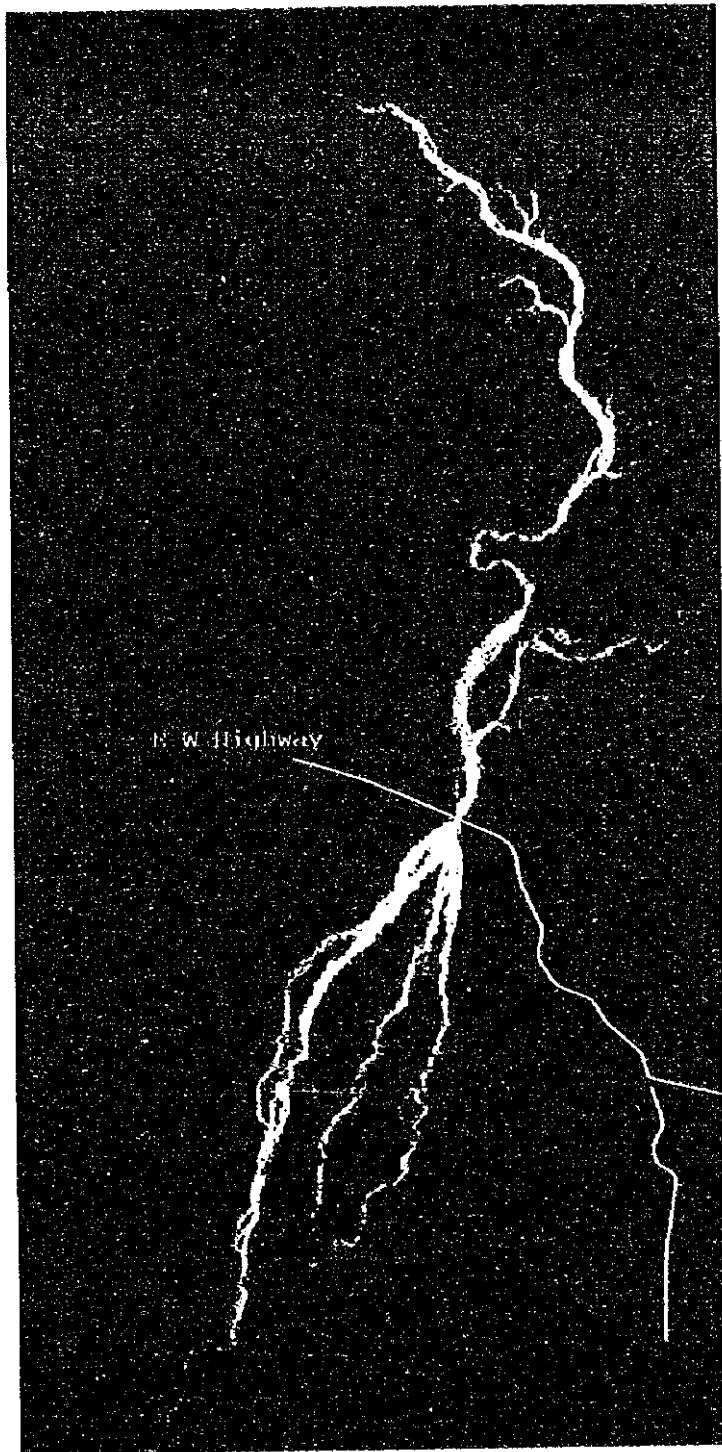| RESEARCH REPORT ON THE INVESTIGATION OF LANDSLIDE AND SOIL EROSION IN NEPAL USING REMOTE SENSING TECHNOLOGY	Figure 7.12	Change of deposition in the floodplain for the period 1993-95
	JAPAN INTERNATIONAL COOPERATION AGENCY	

construction of a dike in the eastern bank of the river, just above the bridge. The newly activated river channel identified on 1977 image below point X is not active in 1993 as shown in the image due to construction of a dike at X. A critical riverbed deposition could have been occurred near point Y in the Figure 7.12, where the channel has been split into two creating a new active sediment transport channel. Originate of this new channel can not be considered as a consequence of the dike at X as the deviation has been taken place few kilometers from the location of the dike. The deviation could have taken place due to topographical changes in the riverbed during the marginal stream flow where the deposition could be very high. Similar explanation could be made to the division of the riverbed identified on the 1977 image in the most eastern river channel just below the Highway. As a whole, it could be said that the floodplain was much active during the 1973 to 79 period than the next 16 years.

There is no much difference was observed between 1993-95 time span within the floodplain. Few newly deposited areas are visible in the lower part of the most eastern sub-stream, and a decrease was observed for its counterpart. This could be an indication of the increasing activity in the eastern side of the floodplain due to continuos deposition in the west side. Limited time span hinder concrete discussion on this matter, but few field visit to further investigate the riverbed topography of this area would be worth to consider. It could be said that the riverbed topography of the floodplain just below the Highway has to be monitor to mitigate the direction of planform deviation of the river channel.

7.3 Typicality of Ratu Watershed in the Siwalik Region

Extrapolation of the study results over the Siwalik region was evaluated by comparing the deposition process taken place in another watershed in the region. Maraha watershed situated few kilometers west of the Ratu watershed was selected for comparison. The Maraha river originates from the Siwalik
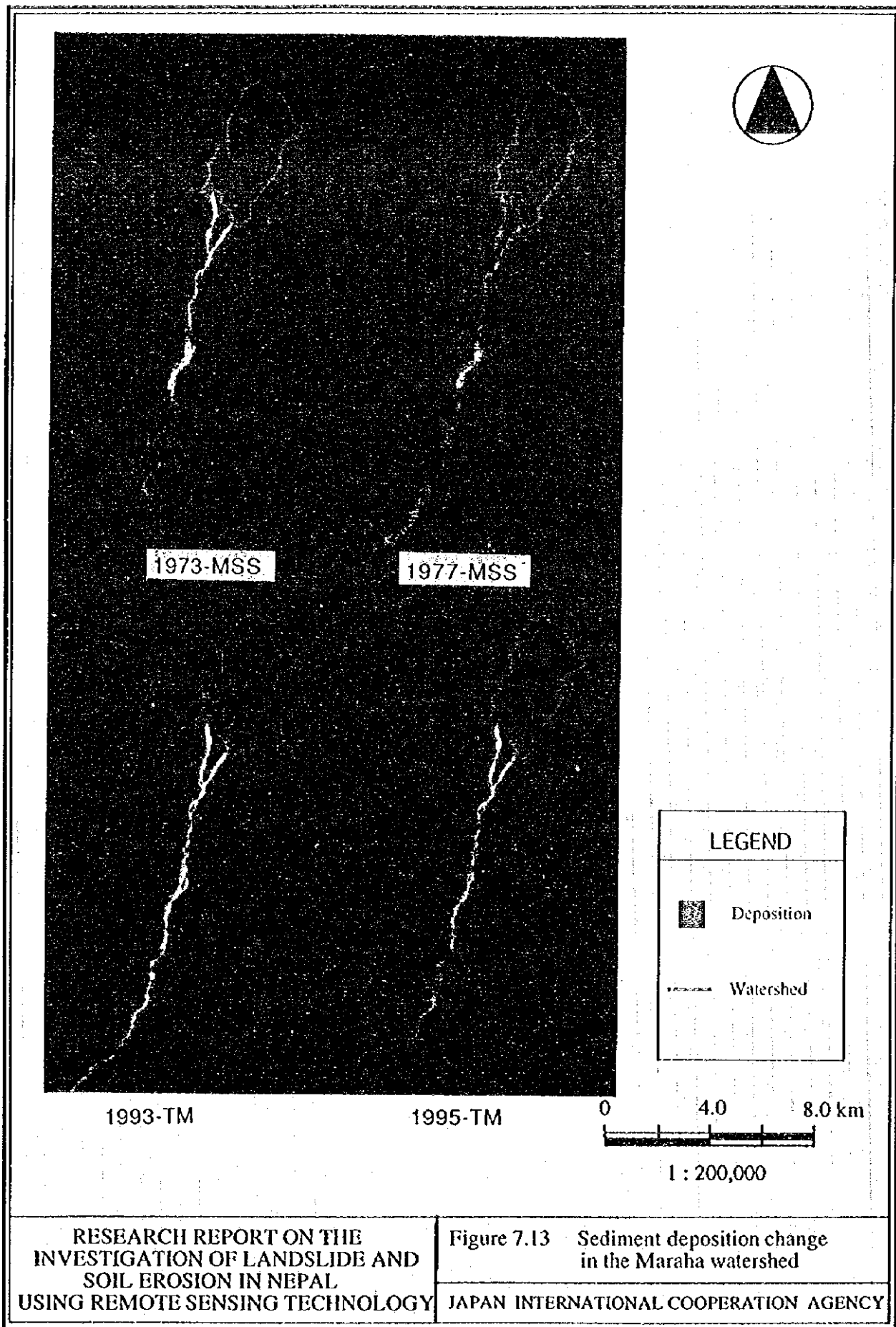
region, and the geological characteristics are almost similar to Ratu watershed. The total area of the watershed is only about 38.3 m^2. Due to relatively small area of the watershed and the steep nature of the topography, the produce sediment as a result of a soil slump or surface erosion is readily available for transport during the rainy season. Hence this river can also be geormorphologicaly categorized into two regions similar to Ratu river; transfer region and lowland region.

Table 7.5 Sediment deposit and change in the Maraha watershed

	1973 sq. km	1977 sq. km	1993 sq. km	1995 sq. km
Upper	0.1179	0.0945	0.6813	0.5427
Floodplain	6.5349	10.1916	8.8290	6.8679

Satellite data derived sediment deposition of the Maraha river is shown in Figure 7.13. The sediment deposited floodplain area is relatively larger when compared to watershed area, but limited to the riverbed. Table 7.5 shows the state of the deposit in the Maraha watershed for the upper stream and floodplain. As in the Ratu watershed the sedimentation is increasing in upper reach. The change is relatively small before 1977, but have increased considerably afterwards. The 1977 floodplain change is similar to that of Ratu watershed showing dramatic increase in the period 1973 to 77. There is a decrease in the time period between 1993 and 1995, and this could be due to 1993 flood event. As there is only one stream is present in this watershed, specifically in the floodplain, the sedimentation is limited to riverbed and its surrounding.

The comparison of the sedimentation in the two watershed are graphically shown in Figure 7.14. Both of the watershed showed similar trend in deposition except for the year 1995. On this comparison it could be said the sediment deposition pattern of Maraha watershed is similar to that of Ratu

1973-MSS   1977-MSS

1993-TM   1995-TM

LEGEND

Deposition

Watershed

0   4.0   8.0 km

1 : 200,000

RESEARCH REPORT ON THE INVESTIGATION OF LANDSLIDE AND SOIL EROSION IN NEPAL USING REMOTE SENSING TECHNOLOGY	Figure 7.13 Sediment deposition change in the Maraha watershed
	JAPAN INTERNATIONAL COOPERATION AGENCY

watershed, and satellite data can be used for estimation of sedimentation and planform change of river channels in the Siwalik area.
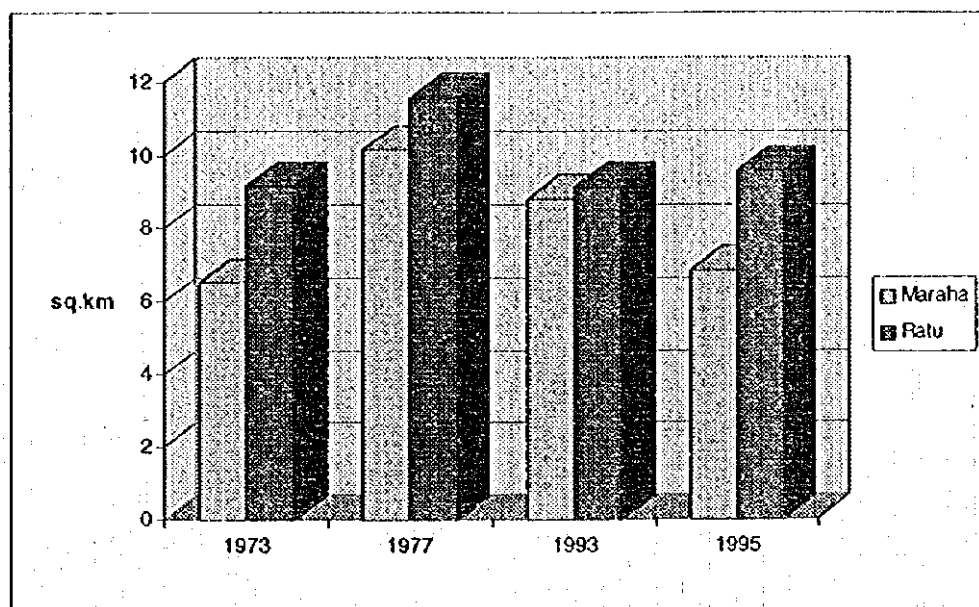

Figure 7.14 Graphical interpretation of sediment deposition changes in Maraha and Ratu watersheds

7.4 Dominant Land cover in the Ratu watershed and the Floodplain

Satellite data was used to estimate the dominant land cover in the present study area, both in the watershed and the down stream floodplain. In general the use of satellite observations in land cover mapping is largely explored and the potentials have been identified. Present attempt was not more than a follow up of methods that have been largely presented and published, but to evaluate the mapping accuracy and applicability to Ratu watershed as the land cover is highly heterogeneous in the area.

Initial attempt to use the 1995 Landsat TM data for land cover mapping was not satisfactory due to spectral similarity of uncultivated lands and some of the deposited areas. Most of the crop lands in the vicinity of the floodplain of the

Ratu river are not cultivate during the dry season, where they resembles to bare lands. Landsat TM spectral response pattern of these lands was similar to spectral response patterns of sediments hindering proper delineation of rain fed crop lands from sediments. Further, though there was a distinguishable spectral pattern for old riverbed for all the scenes facilitating the classification of to delineating old and recent sediments, the similarity of their spectral response pattern with that of the abandoned crop and paddy fields hampered the classification. To avoid these difficulties and increase the classification accuracy it was decided to use two dates datasets, one acquired in wet season, and another representing dry season. It was assumed that this combination would make it possible to delineate the crop and other bare lands as most of the crop lands are cultivated during and after the monsoon rain. In the present study two IRS-LISS datasets, acquired in 1994 November and 1995 March were used for this process. With reference to aerial photographs of 1992, and helicopter observation of 1995, reference areas were defined and classification was carried out using both the satellite datasets based on Supervised Classification method. The resulted land cover map is shown Figure 7.15. The sediment, old riverbeds, forest cover and rain fed crop lands has been classified satisfactorily. Further it was possible to map paddy fields that are distributed below the sedimentation area of the floodplain. Attempt to delineate the houses was not very much successful due to scattered nature of the house distribution, but some areas can be identified. The results show that two seasons satellite data will produce better results in land cover classification in this area due to presence of very high heterogeneity in the spectral response patterns.
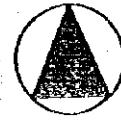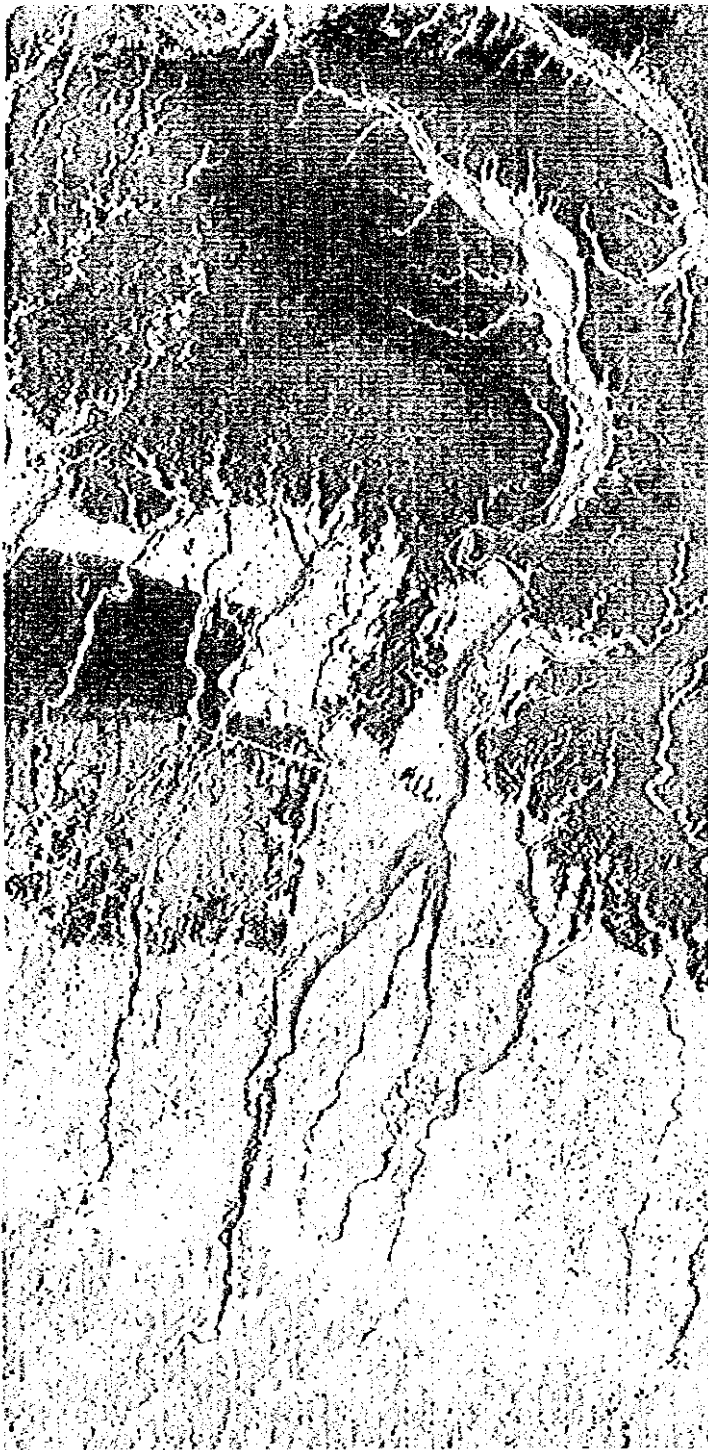
LEGEND

- Forest (Hi-Density)
- Forest (Low-Density)
- Paddy
- Grass land
- Crop 1
- Crop 2
- New Deposit
- Old Deposit
- Houses
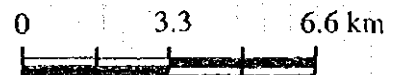
0   3.3   6.6 km

1 : 165,000

RESEARCH REPORT ON THE INVESTIGATION OF LANDSLIDE AND SOIL EROSION IN NEPAL USING REMOTE SENSING TECHNOLOGY	Figure 7.15 Satellite data derived land cover map of the Ratu watershed
	JAPAN INTERNATIONAL COOPERATION AGENCY

CHAPTER 8

SOIL PRODUCTION ESTIMATION BY REMOTE SENSING

CHAPTER 8 SOIL PRODUCTION ESTIMATION BY REMOTE SENSING

It was observed in the previous chapter that the Ratu river is active in transporting and depositing of sediments in the floodplain as well as on the riverbed itself. Observations were made merely for very short geological time span, from 1973 to 1995, but these two dates satellite datasets showed that the sediment area has been increased from 5.1768 to 5.4468 sq. km, accounting 5% of the deposited area of 1973 for the 22 year period. This percentage accounts only for the surface change, and may not reveal the clear picture of the activity as the depth of the deposition is not observable on satellite data. Though this information may not directly be used in to evaluation the rate of deposition or the denudation, the estimates reveals that the soil erosion is active for some years in the Ratu watershed.

8.1 Outline of the Soil Erosion Model

It has been documented that the alluvial deposit in the Ganges Plain extends to a depth about 5000 meters from the sea level (Ives, 1989). Also, it has been shown that the Kosi river has shifted its planform more than 100 km. during the last 250 years, (Summerfield, 1991). These phenomena are evident for massive erosion and deposition in Himalayan region for past millions or more years, (Ives, 1989).

These information reveals that the soil erosion in this region could be considered in two main themes; tectonic activities, and water erosion. The tectonic activities are related to the geology and the geomorphology of the region, and the water erosion is induced by the rainsplash. The geological reasons are yet to define precisely when quantifying erodibility and spatial modeling of soil production in this area due to lack of proper records on soil slumps, landslides and earthquakes. Also, tectonic activities are rather a continental process and may not be evaluated in a micro level watershed. On the other hand, water erosion is more regional and can be considered in micro

scale but lack of field measurements on precipitation and runoff could hinder the application of most of the empirical soil erosion models. Current soil erosion models from Universal Soil Loss Equation to others developed by various authors are results of extensive field observations. Care has to be taken when using these models as they are highly location dependent, and subjected to the characteristics of the place where the observation area made. Further, most of these equation requisite long term rainfall records, and measured denudation rates under different land use conditions.

Comparing the availability of practical models, information required for model estimation with the physical phenomena of soil erosion in the Ratu watershed, utilization of a model that incorporate rainfall data is questionable. The other factor that decide the rate of soil erosion in this watershed is the surface topography, hence a model that relate the surface topography was considered for erosion estimation in the Ratu watershed.

Honda, 1993 proposed the method given below for soil erosion in mountainous region by incorporating surface gradient. He has demonstrated its accuracy applying in a well monitored watershed in Japan. The annul denudation E can be estimated as;

$$E = E_{30}\left(\frac{S}{S_{30}}\right)^{0.9} \qquad\qquad (8.1)$$

Where E_{30} is the rate of denudation at a slope of 30°

S gradient of the surface point under consideration

S_{30} tan(30°)

This model is defined and tested with satisfactory results in the Matsuki watershed in Tochigi Prefecture, Japan. Forest degradation has been taken place in this watershed due to copper mining, and forest restoration, and soil conservation works have been started in 1957. Long term information on precipitation, runoff, characteristics of forest cover, level of regeneration have been collected and used in developing the model defined in equation 8.1. As

the land cover of Ratu watershed is also dominated by forest lands, degraded forest lands, and crop lands, this model may satisfactorily used in estimation of denudation and the total soil loss in this watershed. The denudation factor has to be identified for each spatial location of the watershed or has to measure in well distributed points to apply the model as it is. This is not realistic even in a well monitored watershed, hence an indirect measurement of the denudation factor using satellite measured vegetation index is suggested. In practice, a relationship is established using rate of a surface cover in the interested study area for which the denudation is clearly defined. As the relationship between denudation and NDVI is critical in this method, it is required to identify the potential of NDVI in representing the state of the forest degradation in the interested watershed.

8.2   Land Degradation Assessment by Vegetation Index

Vegetation index is a numerical number that is generated by a combination of spectral bands of a remote sensor representing some form of relationship to the amount of vegetation in a given image pixel. Most of the vegetation indices are based on empirical evidence and may be partially explained by the basic laws of physics, chemistry or biology. Nearly all of the commonly used vegetation indices are only concerned with red and near-infrared region of the electromagnetic spectrum.

It can be assumed that bare soil in an image will form a line in red and near-infrared spectral space and isovegetation lines (lines of equal vegetation) are parallel to soil line. All the isovegetation lines are converge at a single point on the soil line. Presence of isovegetation lines could be due to external factors like differences in irradiance due to surface variability. Therefore, rather than the use of spectral response patterns of red and infra-red bands a ratio will simplify the classification by compensating for external factors. Some of the popular indices are, Normalized Difference Vegetation Index (NDVI), Perpendicular Vegetation Index (PVI), Global Vegetation Index

(GVI), and Soil Adjusted Vegetation Index (SAVI). In the present research work the vegetation index NDVI is used for the analysis as it has been demonstrated the applicability of the index in forest areas. To avoid negative values and for easy handling in image processing software the ratio was calculated using the equation shown in 8.2

$$NDVI = \left[\left(\frac{TMBand4 - TMBand3}{TMBand4 + TMBand3} \right) + 1 \right] \times 100 \quad \text{------------------} \quad (8.2)$$

The main land cover classes within the watershed are; relatively good forest cover, degraded forest, bare ridges account for slumps, soil deposited tributaries and main river and the crop lands. These are observable on the aerial photographs acquired in 1992. Using 1992 November aerial photographs, attempt was made to identify the possibility and the reliability of representing land cover condition in the watershed using NDVI. This was accomplished by comparing the aerial photographs obtained in November 1992 with the NDVI image generated with 1993 March Landsat TM data. The 1:40,000 scale photograph that covers the Ratu watershed was rectified and registered with the created GIS database for facilitate digital comparison. The rectified aerial photograph and the corresponding area of the 1993 satellite data is shown in Figure 8.1, (a) shows the aerial photographs, (b) Landsat TM false color image and NDVI image in (c).

The satellite false color image was created using TM band 2,3,4 assigning blue, green, red for them respectively. Relatively bright red color in the satellite data may represent high vegetation density, and the degraded forest cover can be seen in the lower part of the image in greenish color where the band 4 reflectance has been low. Riverbed is very bright and the crop lands in the vicinity of the river is in light gray.

Degraded mountain ridges, and soil deposited tributaries are very prominent in the aerial photograph. As the photographs are black and white, and due to small scale of photographing, it was quite difficult to differentiate the rate of degradation or the forest cover densities on these photographs. The quality of
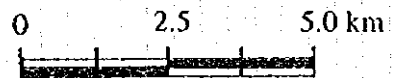
Aerial photographs (a)
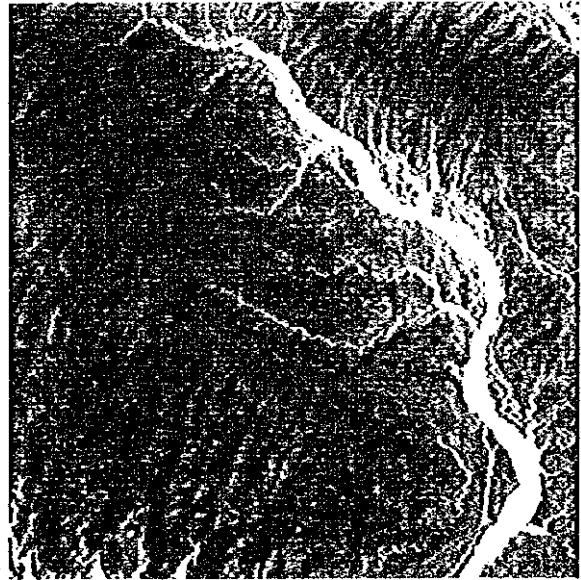
Landsat TM false color image (b)

Landsat TM NDVI image (c)

0   2.5   5.0 km

1 : 125,000

RESEARCH REPORT ON THE INVESTIGATION OF LANDSLIDE AND SOIL EROSION IN NEPAL USING REMOTE SENSING TECHNOLOGY	Figure 8.1 Aerial photographs, false color , and NDVI image of the Ratu watershed
	JAPAN INTERNATIONAL COOPERATION AGENCY

the photograph is comparatively low in differentiating riverbed from crop lands than the satellite data.

The NDVI image, (c) in the same figure depicts differences in the forest cover more clearly. Density of the vegetation is higher in the areas depicted in red color and is low for areas of blue color. The blue gradation, dark to light indicates the change of NDVI and this may account for increase of some form of vegetation. The change of the color from light blue to green then to yellow and finally to different shades of red represent gradual increase of forest cover. NDVI image presents the relative change of vegetation densities, but the absolute values of the densities can not be obtained without the use of reference information.

Using the 1992 aerial photographs, which was scanned for 3.3 meter pixel interval, the density of forest cover in a 100 x 100 meter pixel was estimated. A value of 100 was assigned to bare lands and zero to totally forest covered lands, and the aerial photograph was resampled into 100 meter pixel obtaining the average value of the original pixels that fell within the new pixel area. The digital value of each newly created pixel represented the bare land percentage within the pixel concerned. Subsequently, the Landsat TM NDVI image of 1993 was resampled into same pixel size generating average NDVI for the 100 meter surface area. The relationship of NDVI and the bareland ratio was compared to identify the potential of Landsat NDVI in recognizing the change of forest density. Table 8.1 shows the results after categorizing the bareland ratio into 5% increments.

Table 8.1 Distribution of photograph derived bareland percentage and NDVI values of 1993 Landsat TM

Bareland%	1 to 5	5 to 10	10 to 15	15 to 20	20 to 25	25 to 30	30 to 35	35 to 40	40 to 45	45 to 50
NDVI	114.1	113.1	112.3	111.0	109.9	108.9	107.6	107.7	104.8	103.3
Bareland%	50 to 55	55 to 60	60 to 65	65 to 70	70 to 75	75 to 80	80 to 85	85 to 90	90 to 95	95 to 100
NDVI	101.1	99.7	98.9	97.3	97.7	93.0	94.9	94.9	92.1	88.8

The table shows that the NDVI decreases with the increase of bareland percentage. The highest NDVI for this area was 114 and lowest was 88 for complete forest and 100% bare, respectively. Except for the bareland percentage in the range 75 to 80 the NDVI decreases gradually with the increase of bareland percentage. The irregularity in this range could have been occurred due to averaging effect of 30 meter TM pixels at the time of observation. The relationship is graphically represented in Figure 8.2. The graph shows that the NDVI decreases with the increase of bareland percentage. Except for an undulation in the bareland percentage 70-85%, a negative correlation was observed for the NDVI and bareland percentage. This observation shows that NDVI can satisfactorily be used for represent the land degradation in the Ratu watershed.
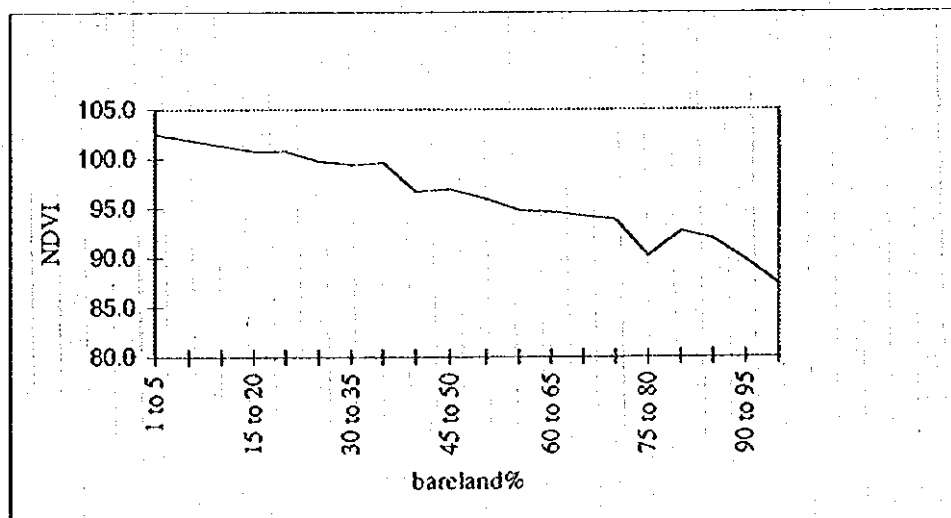

Figure 8.2 Distribution of bareland% and the NDVI values of Ratu watershed

Consequently, the application of NDVI for identification of denuded ridges was attempted. The helicopter photographs obtained during the field visit showed the state of degradation in the mountain ridges, and it was investigated whether those degradation can be quantified using the satellite derived NDVI images. Some of the helicopter photographs were scanned, rectified and compared with NDVI image of 1993. Figure 8.3 and Figure 8.4 shows a set of
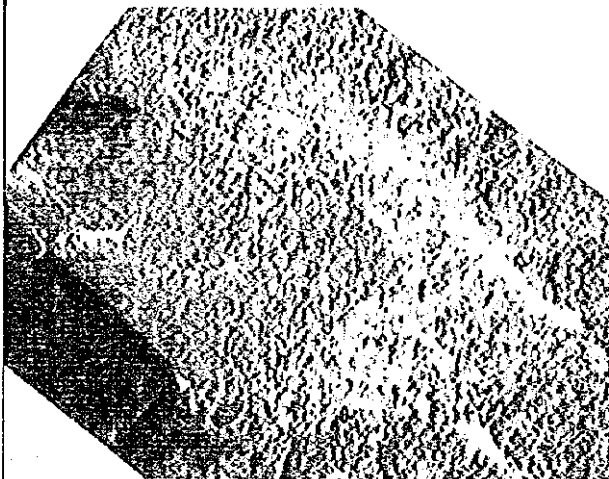
Photograph acquired helicopter flight (a)

Landsat TM natural color image (b)

Landsat TM NDVI image (c)

0   110   220 m
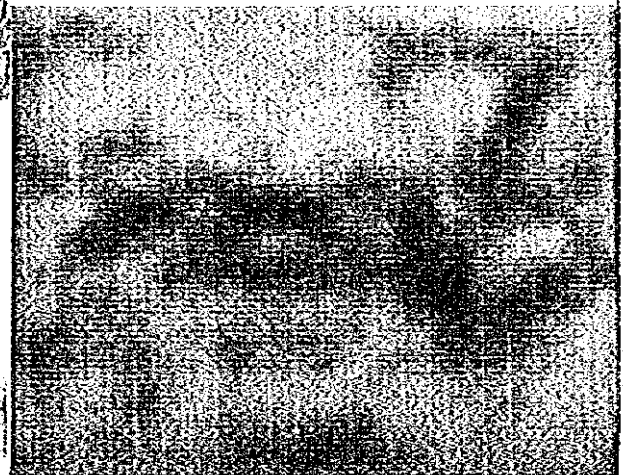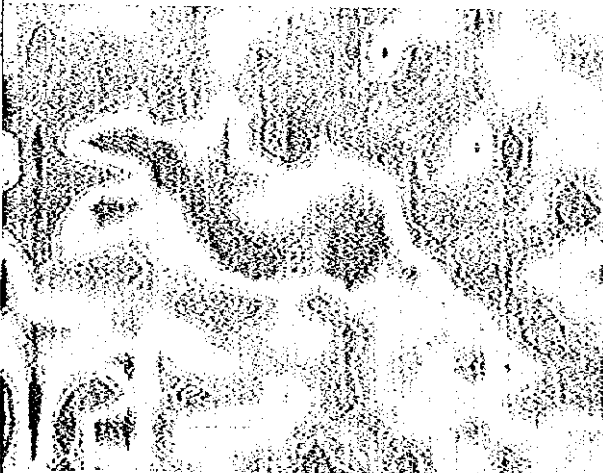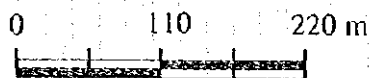
1 : 5,500

Integration of NDVI and helicopter photograph interpretation (d)

RESEARCH REPORT ON THE INVESTIGATION OF LANDSLIDE AND SOIL EROSION IN NEPAL USING REMOTE SENSING TECHNOLOGY	Figure 8.3 Comparsion of helicopter observation with 1993 NDVI image
	JAPAN INTERNATIONAL COOPERATION AGENCY

Photograph acquired helicopter flight (a)

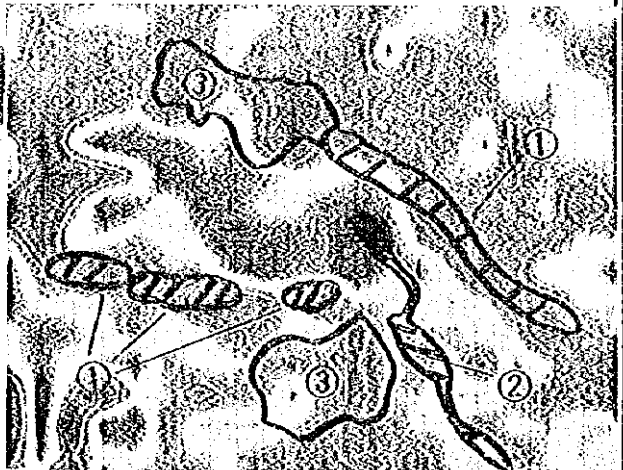Landsat TM natural color image (b)

Landsat TM NDVI image (c)

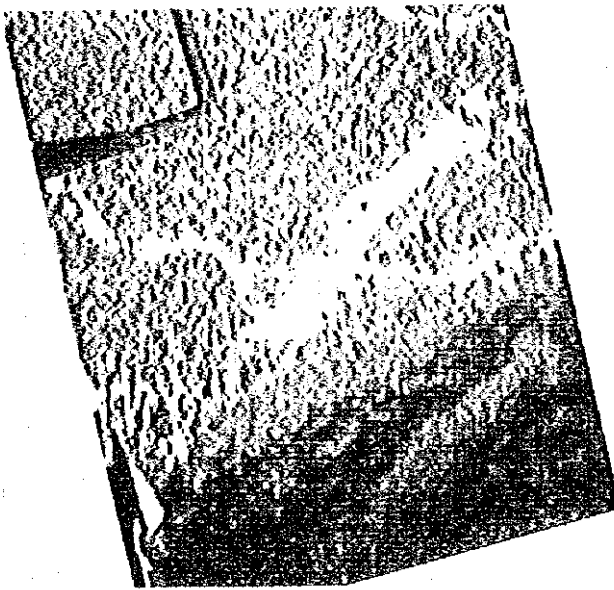0   150   300 m

1 : 7,500
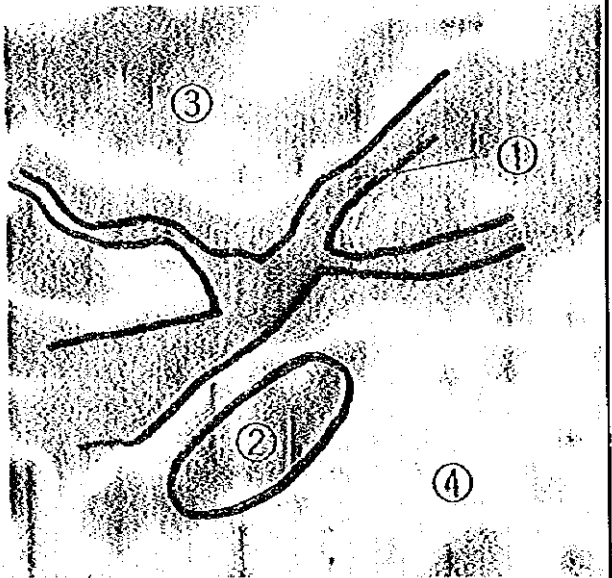
Integration of NDVI and helicopter
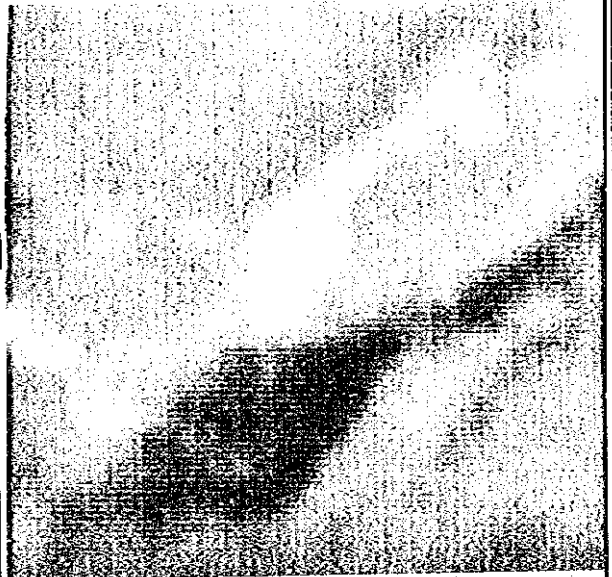photograph interpretation (d)

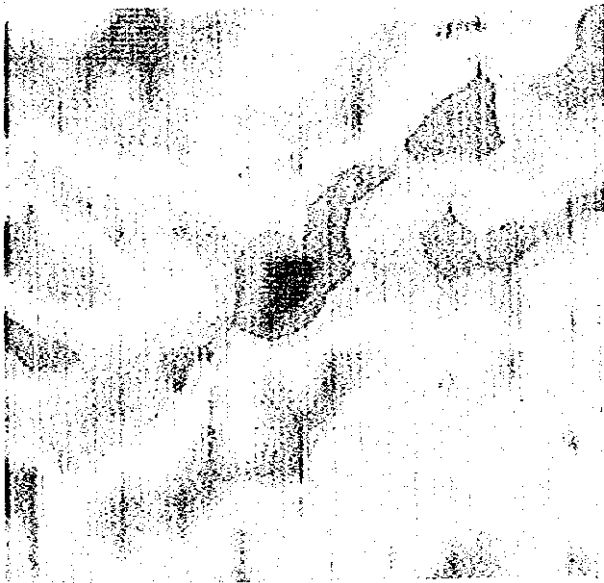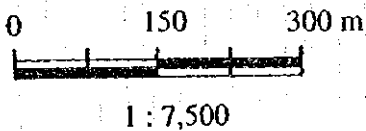| RESEARCH REPORT ON THE INVESTIGATION OF LANDSLIDE AND SOIL EROSION IN NEPAL USING REMOTE SENSING TECHNOLOGY	Figure 8.4 Comparsion of helicopter observation with 1993 NDVI imgae
	JAPAN INTERNATIONAL COOPERATION AGENCY

photographs representing same spatial location of the Ratu watershed. Image (a) is the photograph acquired during helicopter flight, (b) Natural color image of TM 1993, (c) corresponding NDVI image and the (d) is integration of NDVI and helicopter photograph interpretation, respectively. Approximate scales of the images are shown for assess the viable sensor resolution.

The degree of forest density increases from blue to green, then to yellow and finally to red. The different gradations show the continuity of the increase. Highest forest cover is represented by red color, and the lowest by blue.

In the Figure 8.3, most of the degraded ridges can clearly be identified with blue region on NDVI. The sparsely grown forest areas, 3 in the figure shows relatively smaller NDVI and the distribution of the values could be taken as the density index. The red color in the center of NDVI represents the dense forest cover in the photograph. The tributary, 2 is not clearly visible on the NDVI image, specially near the densely forested area. This could be due to the resolution of the sensor and mixed land cover that could present in a single pixel of TM data. The interpretation of NDVI is much easier and the difference forest classes are enhanced in NDVI than in natural color image.

In Figure 8.4, the tributary is clearly visible in NDVI, and also in natural color image. Densely forested area is clearly visible in NDVI, and area 3 can be interpreted as sparse vegetation, but its surface coverage is higher than area 4 according to NDVI interpretation. This is not clearly visible in natural color image, or in photograph.

The foregoing discussion comparing aerial photographs and helicopter photographs with satellite data showed that the remotely sensed data can satisfactorily be used in identifying degraded forest, denuded ridges and silted tributaries and main streams. The continuous nature of NDVI facilitate the interpretation of forest density more realistically, than classifying the forest cover into discrete density classes. The interpretability is hampered by the resolution of the sensor, but in some locations the degraded ridges were clearly visible even their spatial extent is less than the resolution of the sensor.

8.3 Estimation of Soil Yield in Ratu Watershed

The reliability of identification of degraded land using Landsat TM derived NDVI was discussed in the previous section, and found that this index can satisfactorily be used in estimation of land degradation. The estimation of soil yield in the Ratu watershed was carried out based on the equation describe 8.1. It was explained in section 8.1 that the denudation rate is required to use the equation and these values for the present watershed was acquired from published literature. Table 8.2 gives denudation rate in the Himalayan region and in a regulated watershed in Japan where the Honda, 1993 developed the equation 8.1.

Table 8.2 Land denudation for some areas in Nepal and Japan

Description of the site	Rate tons/km^2/year	Reference
Siwalik: East Nepal, S-aspect, sandstone foothills, landuse from forest to grazing lands	780-3,680	Chatra, 1976
Siwalik: Far West Nepal, S-aspect, sandstone foothills		
Degraded Forest	2,000	Laban, 1978
Degraded forest, gullied land	4,000	Laban, 1978
Severely degraded, heavily grazed	20,000	Sakya
Middle Mountains: Katmandu valley, steep slopes	800	Laban, 1978
Japan: Asio region in Tochigi Prefecture for 30° slope		
Crop lands	20 mm/year	Honda, 1993
Grasslands	1 mm/year	Honda, 1993
Forest	0.1 mm/year	Honda, 1993

Values for East Nepal, 780-3680 tons/ km^2/year represent about 0.4 mm/year, and 18.5 mm/year, respectively assuming the density of the sediment is 2 g/cm^3. These figures are for extremes of the Eastern Siwalik area.

In order to evaluate the soil production, the denudation rate for each pixel has to be estimated using reference information given in Table 8.2 or otherwise.

The values obtained by comparing aerial photographs in the Table 8.1 represent the average NDVI for particular bareland ratio interval. The highest value of NDVI, 114 was considered as the representation of forest cover in this area, and the lowest value as the representation of bareland. Attempt was made to establish the denudation rate of Ratu watershed comparing the Middle Mountain range forest cover for which Laban, 1978 identified the erosion rate of 800 tons/km^2/year, Table 8.2. Visually observing Landsat TM image of 1993, forest cover was identified in the Middle Mountain, north of Sindhulimadi. Sample area was defined and average of forest cover was calculated. It was found that the average NDVI value for forest in this region is 135, representing higher forest coverage than that was in the Ratu watershed. Comparison of other satellite datasets showed that the forest cover in the area selected was not degraded. Therefore, the denudation of this cover area was considered very less, and referring to Table 8.2 the denudation rate of this forest cover was defined as 0.4 mm/year (800 tons/km^2/year). Rate of denudation for the forest land in the present watershed was considered as 2 mm/year (4000 tons/km^2/year), highest documented for Eastern Nepal, and for bareland 20 mm/year, same as the denudation rate used in Japan. All of these denudation rates are assumed to be for land surfaces with 30° slope angle. In order to estimate the soil yield for the whole watershed, a relationship was considered for denudation and NDVI, (Honda, 1994). He has demonstrated that NDVI is related to common logarithm of the denudation rate. The interpretation of denudation with respect to NDVI can be carried out as shown in Figure 8.5.

Using the relationship in the figure, the denudation was calculated for a given NDVI value, hence the rate of denudation is known for any pixel in the watershed with respect to 1993 land cover condition. The other factor that is required for soil yield estimation is the slope gradient, and it was calculated from the digital elevation data. Figure 8.6 and 8.7 shows the general trend of the elevation in the watershed, and the distribution of slope. Soil yield with respect to 1993 land cover was estimated as 321,156 cubic meters per year.
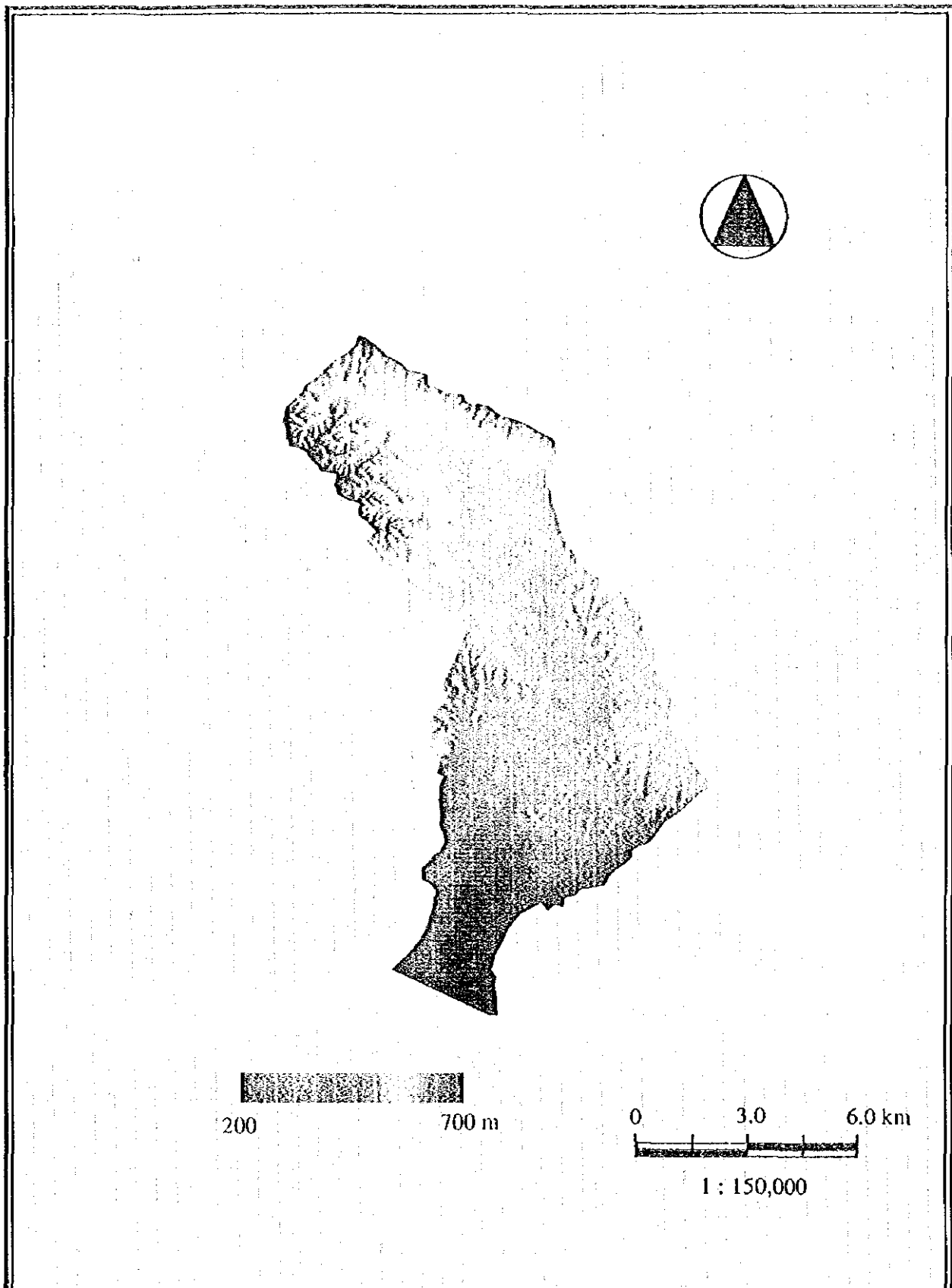
200   700 m

0   3.0   6.0 km

1 : 150,000

RESEARCH REPORT ON THE INVESTIGATION OF LANDSLIDE AND SOIL EROSION IN NEPAL USING REMOTE SENSING TECHNOLOGY	Figure 8.6 Elevation distribution of the Ratu watershed
	JAPAN INTERNATIONAL COOPERATION AGENCY
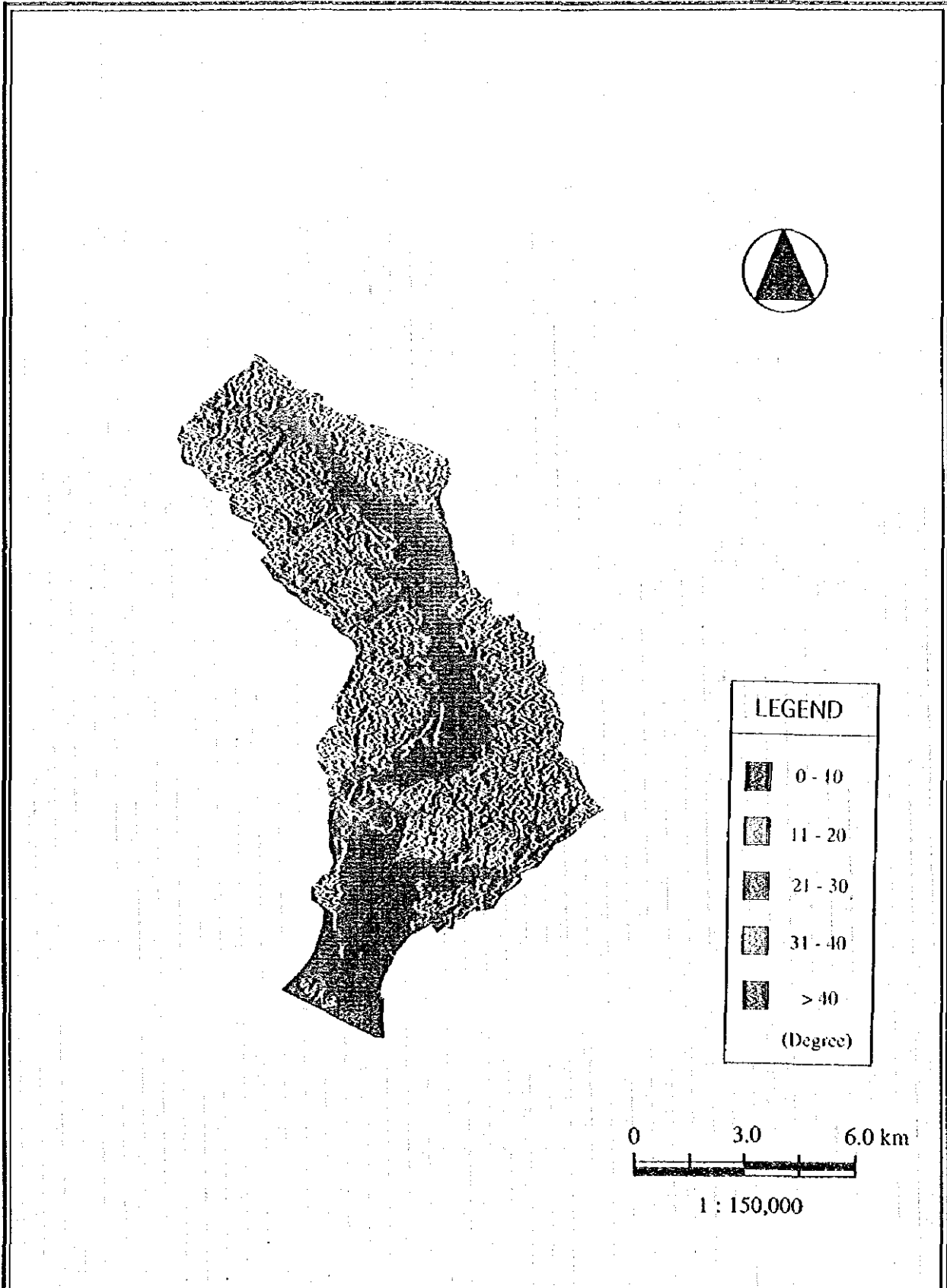
LEGEND

▨	0 - 10
▨	11 - 20
▨	21 - 30
▨	31 - 40
▨	> 40

(Degree)

0   3.0   6.0 km

1 : 150,000

RESEARCH REPORT ON THE INVESTIGATION OF LANDSLIDE AND SOIL EROSION IN NEPAL USING REMOTE SENSING TECHNOLOGY	Figure 8.7 Slope data created by GIS using topographical JAPAN INTERNATIONAL COOPERATION AGENCY
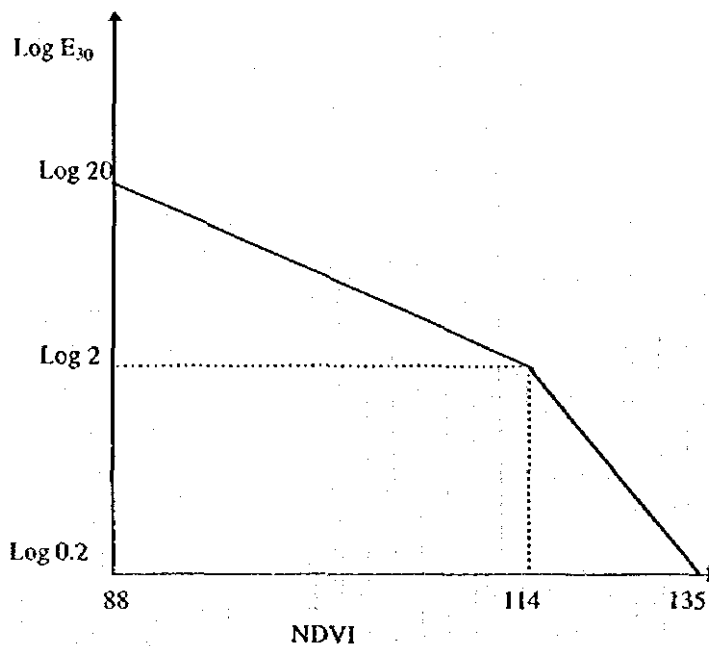
Figure 8.5 Calculation of rate of denudation using NDVI

The average denudation of Ratu watershed according to this estimation is 3.89 mm/year. The distribution of the potential of soil yield of the Ratu watershed is thematically shown in Figure 8.8. The color representation is similar to that of NDVI, where red for highest potential and blue for the lowest soil yield areas.

8.4 Temporal Remote Sensing Data for Soil Yield Monitoring

In the preceding section estimate was carried out for potential of soil production on the basis of 1993 land cover of the Ratu watershed, specifically with respect to forest density and the surface slope of the area. In this section, estimation was carried out for soil yield potential in the watershed for the dates 1973, 77 and 1995.

Considering no appreciable change of the topography during the 22 year period from 1973 to 95 , proposed equation for soil erodibility was used for estimation of the denudation rate and the volume of the soil production based on NDVI derived forest cover densities. Reliable data for comparison with
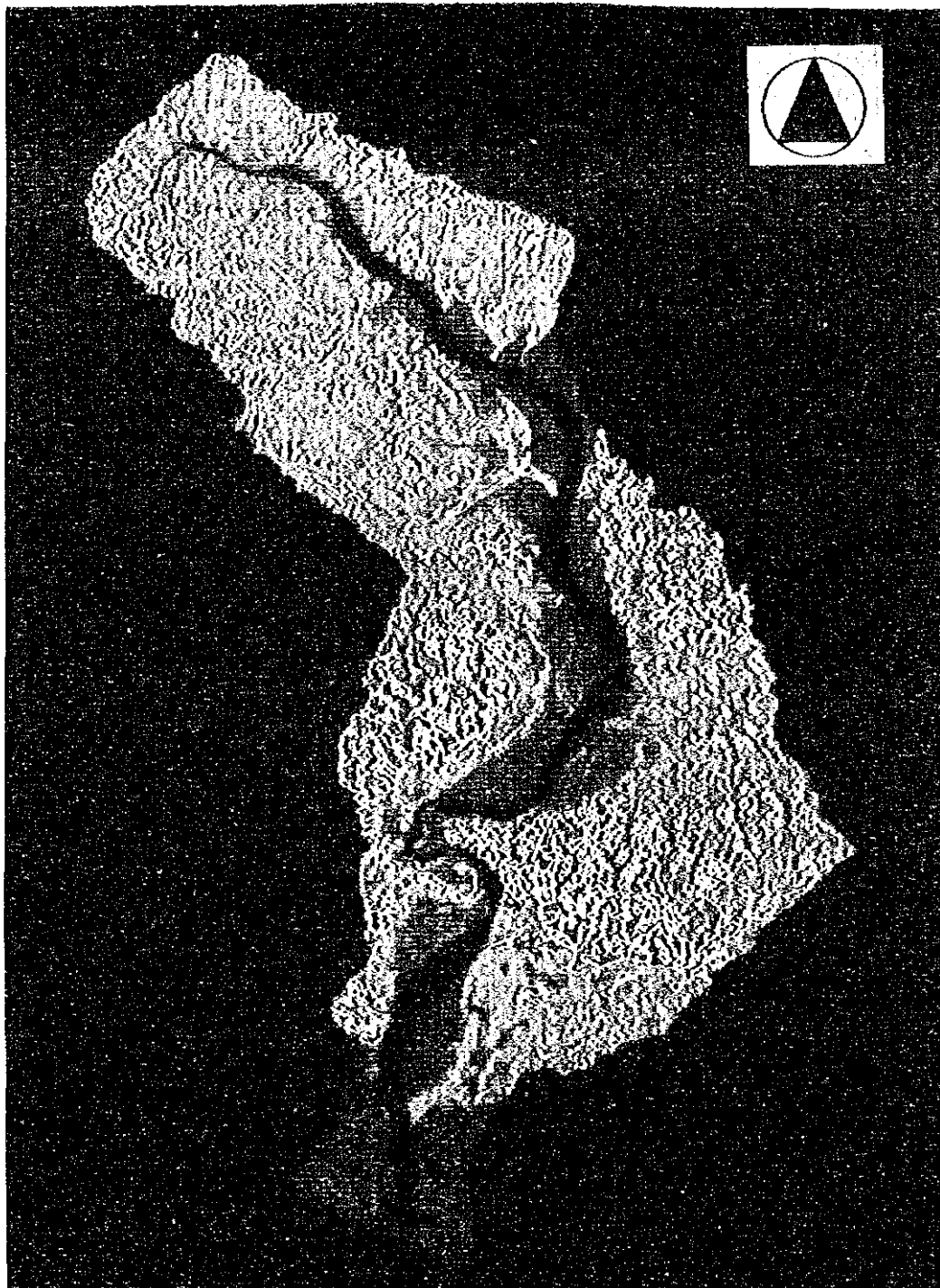
0   80 m³

0   2.0   4.0 km

1 : 100,000

RESEARCH REPORT ON THE INVESTIGATION OF LANDSLIDE AND SOIL EROSION IN NEPAL USING REMOTE SENSING TECHNOLOGY	Figure 8.8 Potential of annual soil yield in the Ratu watershed reference to 93 land cover
	JAPAN INTERNATIONAL COOPERATION AGENCY

satellite data of 1973, 77 was not available in order to establish a relationship of the forest density at the time of satellite pass with the corresponding NDVI images. On the other hand, if ground truth data, such as photographs are available the use of satellite data is unwarranted. One of the objectives of the present work is to recognize a method that can be used to evaluate the erodibility and the soil production in the Siwalik region using satellite data integrating nominal amount of readily available other information, and investigation of multi-temporal and multi sensor satellite data for soil erosion modeling. Under this condition attempt was made to use 1993 NDVI as base dataset in establishing the forest cover of 1973, 77 and 1995.

Table 8.3 shows the bareland ratio of 1993, describe in the previous section and the NDVI values of 1973, 77, 95, also the 1993 NDVI values that used for estimate the soil yield in the previous section. Further, the distribution of the NDVI values and the bareland ratio is graphically shown in Figure 8.9.

Table 8.3 Bareland ratio and the NDVI values for four dates satellite data

Bareland%	73	77	93	95
	Mean	Mean	Mean	Mean
1 to 5	124.3	121.3	114.1	102.6
5 to 10	123.7	121.2	113.1	101.9
10 to 15	123.0	120.5	112.3	101.4
15 to 20	122.3	119.7	111.0	100.7
20 to 25	121.1	117.8	109.9	100.8
25 to 30	120.7	117.4	108.9	99.8
30 to 35	119.0	115.8	107.6	99.5
35 to 40	119.8	116.8	107.7	99.5
40 to 45	118.7	115.7	104.8	96.8
45 to 50	114.8	113.8	103.3	96.8
50 to 55	115.1	113.9	101.1	95.9
55 to 60	114.9	113.9	99.7	94.9
60 to 65	111.9	111.1	98.9	94.6
65 to 70	113.9	111.5	97.3	94.3
70 to 75	113.6	112.1	97.7	93.8
75 to 80	109.4	110.1	93.0	90.2
80 to 85	114.1	110.8	94.9	92.7
85 to 90	110.2	110.8	94.9	91.9
90 to 95	107.3	107.9	92.1	89.8
95 to 100	104.0	106.2	88.8	87.4
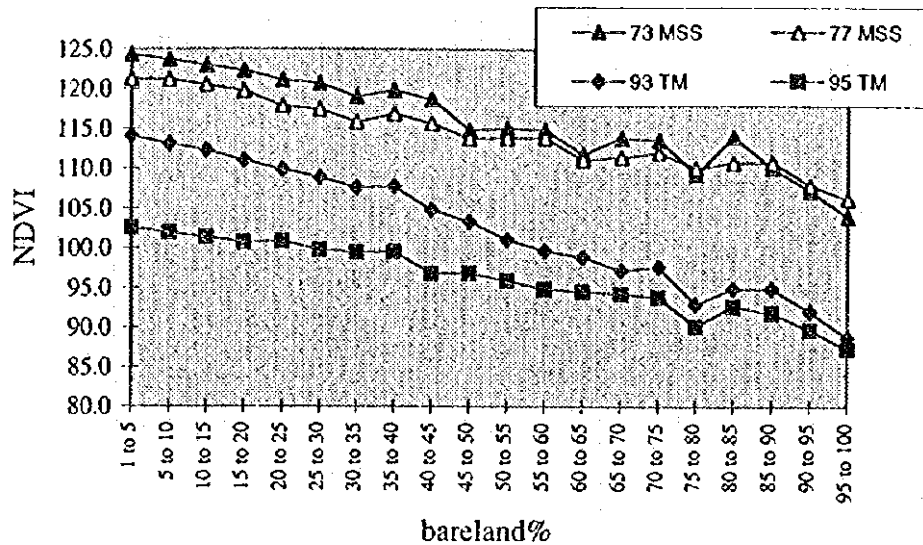
Figure 8.9 Distribution of bareland% and 4 dates NDVI values

The trend was similar for all satellite datasets. The 1995 NDVI showed the smallest values and 73 MSS data showed the highest NDVI values for a given bareland percentage. Further, a shift was observed for MSS and TM datasets and this could be due to spectral resolution of the two different sensors. Totally bareland showed similar values for two sets of TM data, and NDVI values for MSS datasets also converged to a similar value for complete bareland though the MSS and TM values were different in magnitude. The distribution of MSS NDVI values for bareland ratio indicates similar values with small decrease in the 1977 dataset. In contrast to this, the 93 TM showed very high values for totally forested areas compared for 1995. Differences or the irregularities in the two different sensors and four dates observation could be due to following factors;

Internal change in the forest cover

Changes in the forest densities

External factors such as atmospheric condition at the time of observation

Spatial and spectral sensitivities of the two different sensors

The change of high end NDVI values for 1973 and 1993 was 125 and 114 (11), and the change between 93 to 95 was 114 to 103 (11). This difference can not be considered as due to forest cover change as the difference between 1993-95 NDVI values is unrealistic if the different between 1993 to 93 is taken as correct representation of 20 year forest change. Further, for MSS the decreasing trend of NDVI from 73 to 77 has been reversed for the higher bareland cover. Therefore, this discrepancies could have been occurred due to external factors or during the pre-processing of data at the receiving stations.

In order to compare the NDVI values of different sensors that have been undergone different pre-processing it is required to bring them to a similar scale. As observation parameters or the pre-processing parameters were not available, attempt was made to relate them with the 1993 NDVI and 1992 aerial photographs derived bareland ratios, *histogram matching* method was carried out. In this method it is assumed that there are some pixels that have little or no variation in their mean surface reflectance between images. In the present study similar assumption was made in histogram matching, assuming there was spectrally invariable forest cover and non-vegetative areas present in four dates satellite datasets. Having used NDVI image of 1992 Landsat TM dataset as the reference image, NDVI images of 1973, 77 and 95 were transformed to match the distribution of NDVI values with the reference image. The original NDVI images and the transformed NDVI matching with 1993 NDVI image are graphically shown in Figure 8.10 and 8.11. The 1977 dataset showed very high irregularity after transformation, and this effect was due to the atmospheric condition prevailed at the time of satellite pass. A false color image of 1977 showed presence of thin cloud cover covering most of the area. This heterogeneity in the atmospheric property across the scene might have distorted the spectral response from the surface destroying the relative pattern with other datasets. This dataset was excluded from further use for erosion production estimation.
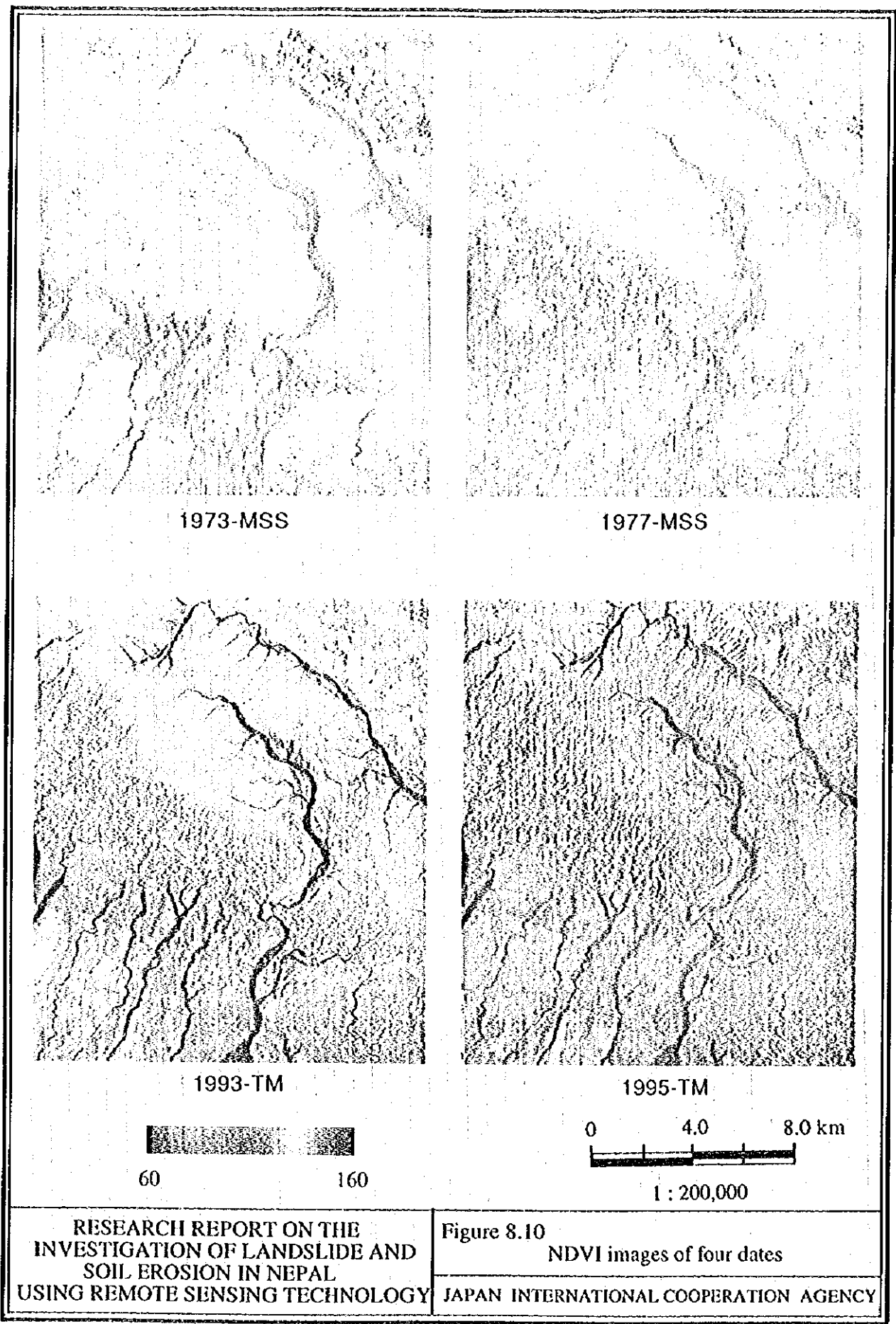
1973-MSS

1977-MSS

1993-TM

1995-TM

60   160

0   4.0   8.0 km

1 : 200,000

RESEARCH REPORT ON THE INVESTIGATION OF LANDSLIDE AND SOIL EROSION IN NEPAL USING REMOTE SENSING TECHNOLOGY	Figure 8.10 NDVI images of four dates
	JAPAN INTERNATIONAL COOPERATION AGENCY
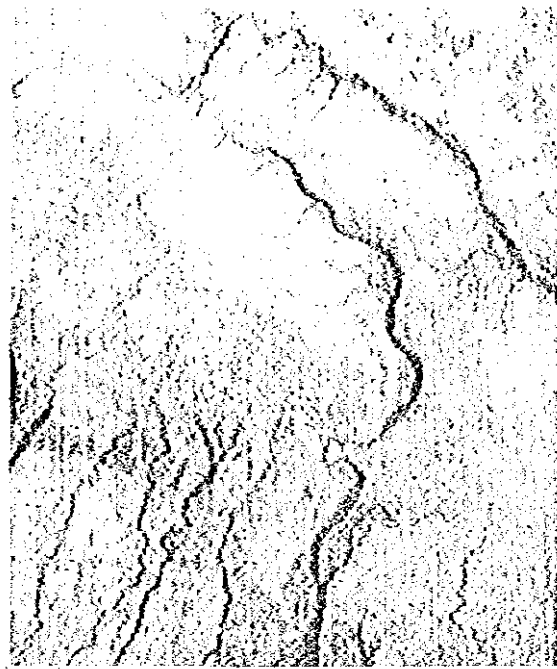
1973-MSS

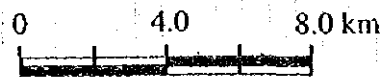1977-MSS

1993-TM

1995-TM

0   4.0   8.0 km

60   160

1 : 200,000

RESEARCH REPORT ON THE INVESTIGATION OF LANDSLIDE AND SOIL EROSION IN NEPAL USING REMOTE SENSING TECHNOLOGY	Figure 8.11 NDVI images after histogram matching reference to 1993 NDVI data
	JAPAN INTERNATIONAL COOPERATION AGENCY

Using the transformed NDVI and the previously established denudation rates for 1993 land cover classes the soil yield was estimated for other dates, and presented in Table 8.4.

Table 8.4 Soil yield and denudation estimate for Ratu watershed

|	1973	1993	1995
Soil Yield m^3	271,110	321,156	293,096
Rate of denudation mm/year	3.29	3.89	3.55

The results obtained showed a gradual increase of land degradation and denudation in this watershed. An average denudation rate of 3.5 mm/year, or 7000 tons/km^2/year observed in this study falls in the extreme end of the publications in the Table 8.2.

8.5   Estimation of Soil Production during 1993 Storm Event

The foregoing section evaluated the annual average soil yield on the basis of land use and the surface topography. The model that used in the evaluation does not include the rainfall data. Due to very limited rainfall in the Ratu watershed where the mean annual rainfall is within 1500 ~ 2000 mm, Figure 8.12, the estimated soil production in the previous section can be considered as a reasonable estimate of annual soil production under normal condition.

The equation 8.1 cannot be used for estimation of soil production during a cloud burst incidence that could bring about 500 mm of rainfall within few hours. One reason for this is that the intensive rainfall could accelerate the surface erosion, but the most important factor is the drastic level of production that can take place as failures described in section 6.1.

Figure 6.4 shows a clear picture of the probable failure types, where the landslide along the banks of the stream, undercutting, or earth topple are some of the main factors that highly contribute to sediment transport from upper watershed during 1993 flood event. In overall, the areas around the sub-

(After Sharma,1995)

0   90   180 km
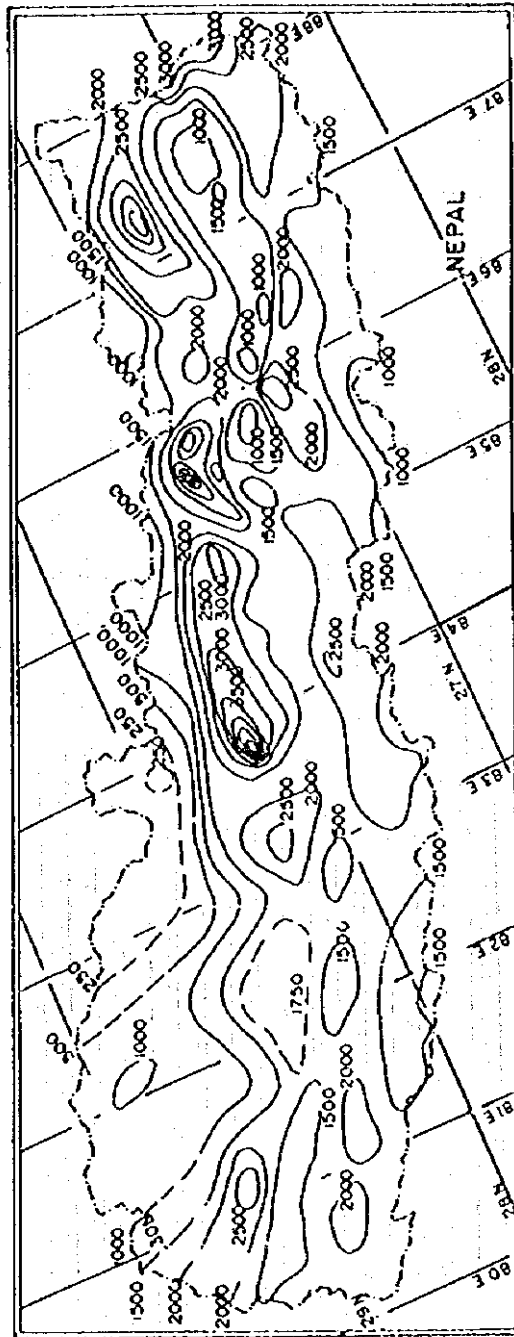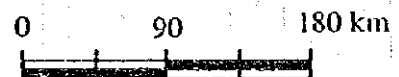
1 : 4,500,000

RESEARCH REPORT ON THE INVESTIGATION OF LANDSLIDE AND SOIL EROSION IN NEPAL USING REMOTE SENSING TECHNOLOGY	Figure 8.12 Mean annual precipitaion (mm. 1971-85)
	JAPAN INTERNATIONAL COOPERATION AGENCY

streams are very much vulnerable to soil erosion during a flood event than other areas where the surface erosion is the main soil production phenomena. Considering these factors it was attempted to modify the equation 8.1 that is used for estimation of annual sediment production to applicable in a flooding event.

It is clear that presence of sub-streams increase the volume of sediment under heavy rainfall. Therefore, inclusion of this topographical parameter into the model was considered for modification of the model.

It was observed that all the sub-streams are not visible in remote sensing images due to sensor resolution and the topographic nature of the area. Figure 8.13 shows the general distribution of a sub-stream in the watershed that is not visible in TM data. Two sub-streams separated by a ridge is shown here. When the ridges are covered with vegetation, the vertical river banks could make the stream undetectable for remote sensors. In contrast to this, the degraded ridges where there is no vegetation leaves the space to catch these sub-streams from the sensor if the resolution permits. According to field investigations explained in section 6.1.2, both of these sub-streams contribute to soil production. As remote sensing data can not acquire most of these hidden streams it was considered to include this topographical information through other source of data.

In order to integrate the distribution of stream and its impact on the soil production in a storm water incident, it was decided to include the density of the sub-stream as a erodible factor in the equation 8.1. Further, the land cover of the sub-stream banks, or on the banks also responsible for the amount of soil slumps, or landslides that can occur in an event, hence the effect due to these two parameters could have a multiplicative effect on the production of soil. Therefore, it was considered a multiplication factor in equation 8.1 that represent the sub-stream distribution within the watershed can compensate for heavy erosion in a storm event. This factor was calculated using the data layers in the GIS database. Soil production was calculated for each sub-watershed using the prediction formulas developed by the field observations.

Length of sub-streams of each of these watershed was calculated through GIS approach.
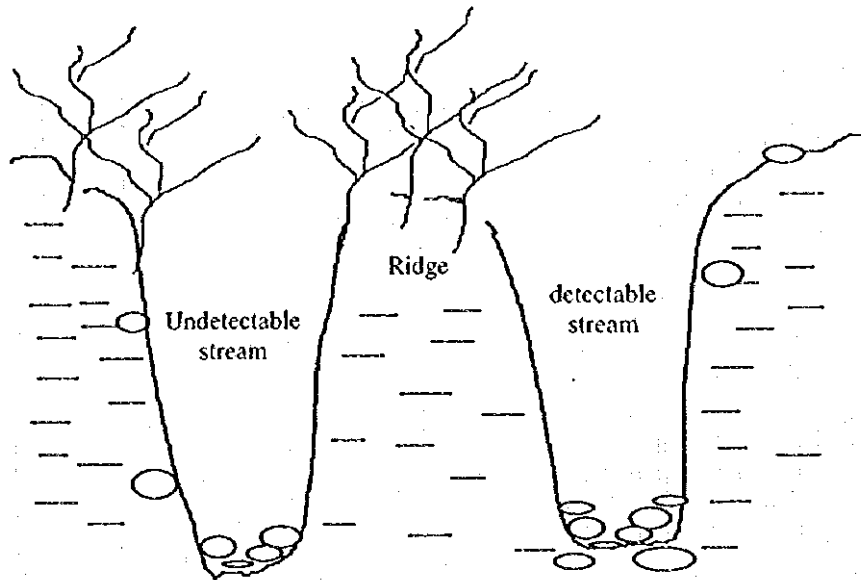
Figure 8.13 Sectional view of sub-streams in the watershed

The correction index for flood event of 1993 (α) was calculated for each watershed depicted in Figure 7.6 as follows;

$$(V_{Total})_i = \sum^{allpixels} E_{30} \left(\frac{S}{S_{30}} \right)^{0.9} \times S_i \times \alpha_i \qquad (8.3)$$

Here $(V_{Total})_i$ is the estimated production of watershed i by field investigation (Chapter 6)

     α_i Topographical factor for watershed i

     S_i $(L_i \times L_i)/A_i$

     L_i Length of streams in the watershed i

     A_i Surface area of the watershed i

     $\sum^{allpixel}$ Estimation of soil production for watershed i using all the pixels that fell in the watershed i

Using the above formula, α_i for each sub-watershed was calculated, and this factor was considered as the topographical factor that represent the contribution to sediment production during a flood event. Using the above factor, soil production of 1993 was re-calculated using Landsat TM 1993 NDVI image resulting 1,980,000 m^3, and this amount is very much closure to the 2.29 million m^3 estimated by field observations. Assuming this *flood event soil factor* can be used in predicting soil production that would result during a storm event given a NDVI image just before a rainy season. The estimation by the model and field estimation was almost agreed with only 10% discrepancy.

CHAPTER 9

CONCLUSION AND RECOMMANDATION

CHAPTER 9 CONCLUSIONS AND FUTURE RECOMMENDATIONS
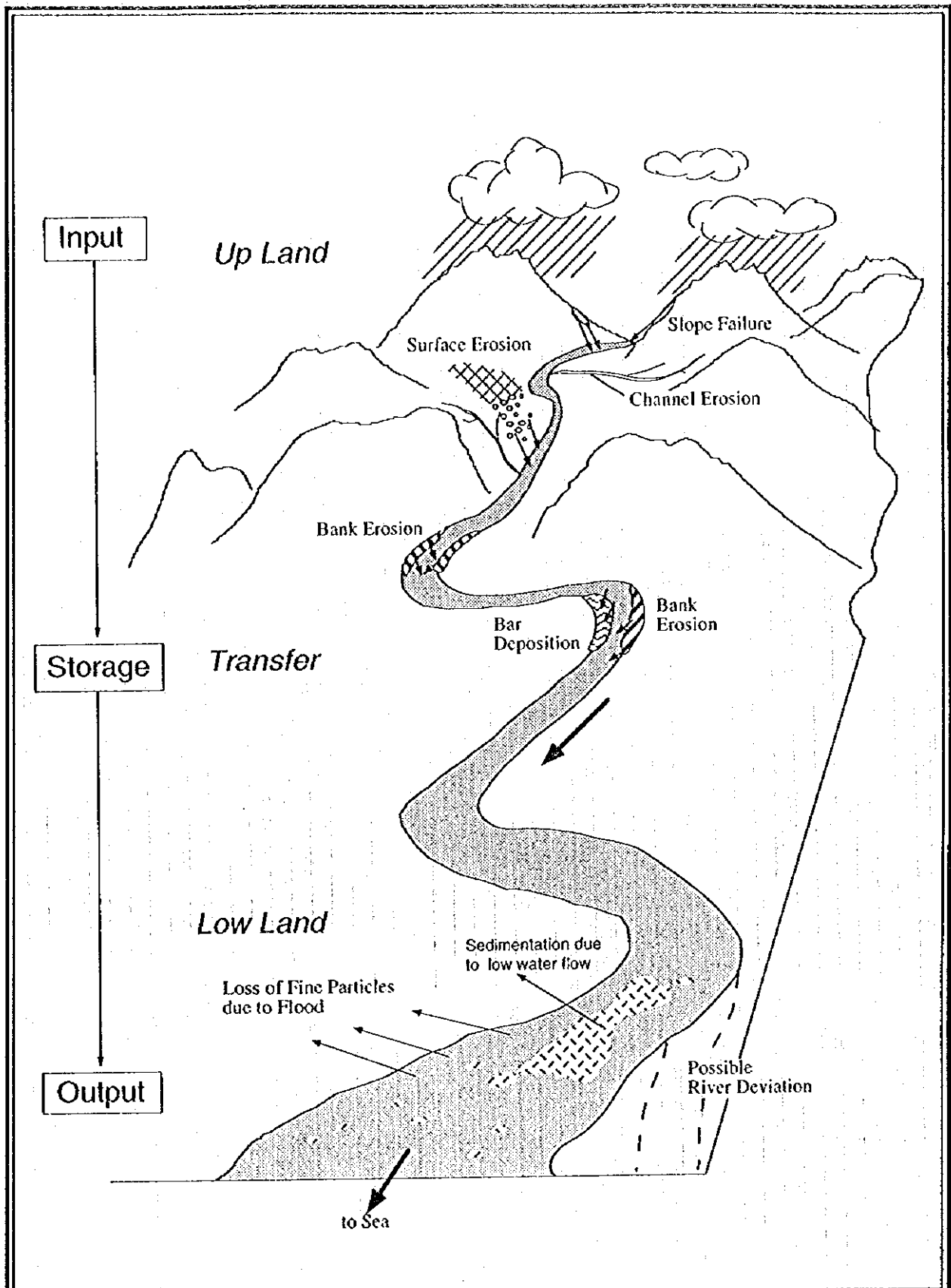
9.1 Results and Discussion

The main aim of the present research work was to establish a methodology that can be used for estimate the soil balance and the production process in the Ratu watershed using satellite remote sensing and GIS technologies. The soil erosion phenomena, its transportation and the deposition in the Ratu watershed that was describe in detail in the chapter six can be illustrated as in the Figure 9.1.

The analysis procedures carried out in this research work can be categorized as shown in Figure 9.2. This shows the flow of the analysis of remote sensing data for extents monitoring, and integration with other information for volumetric evaluation. The figure explains the flow of the data and the process under direct observations from satellite data, and derived outputs using supplementary information for clarity of the whole analysis procedure. Soil production, transportation and deposition was evaluated spatially and volumetrically. Subsequently, a model was formulated to estimate the soil production using spatial estimates carried out by remote sensing data for evaluate the volumetric changes. Annual average soil production was estimated under normal condition using the model that consisted with parameters observable by remote sensing data and topographical maps. Further, this model was modified for estimation of soil production during a flood event. The obtained results can be enumerated as spatial and volumetric as shown below.

Results of Spatial change estimation

* It was possible to estimate the riverbed changes in the upper watershed using satellite data, satisfactorily.

Input

Storage

Output

Up Land

Surface Erosion

Slope Failure

Channel Erosion

Bank Erosion

Transfer

Bank
Erosion

Bar
Deposition

Low Land

Sedimentation due
to low water flow

Loss of Fine Particles
due to Flood

Possible
River Deviation

to Sea

RESEARCH REPORT ON THE INVESTIGATION OF LANDSLIDE AND SOIL EROSION IN NEPAL USING REMOTE SENSING TECHNOLOGY	Figure 9.1 Geomorphological process of soil production and transport
	JAPAN INTERNATIONAL COOPERATION AGENCY
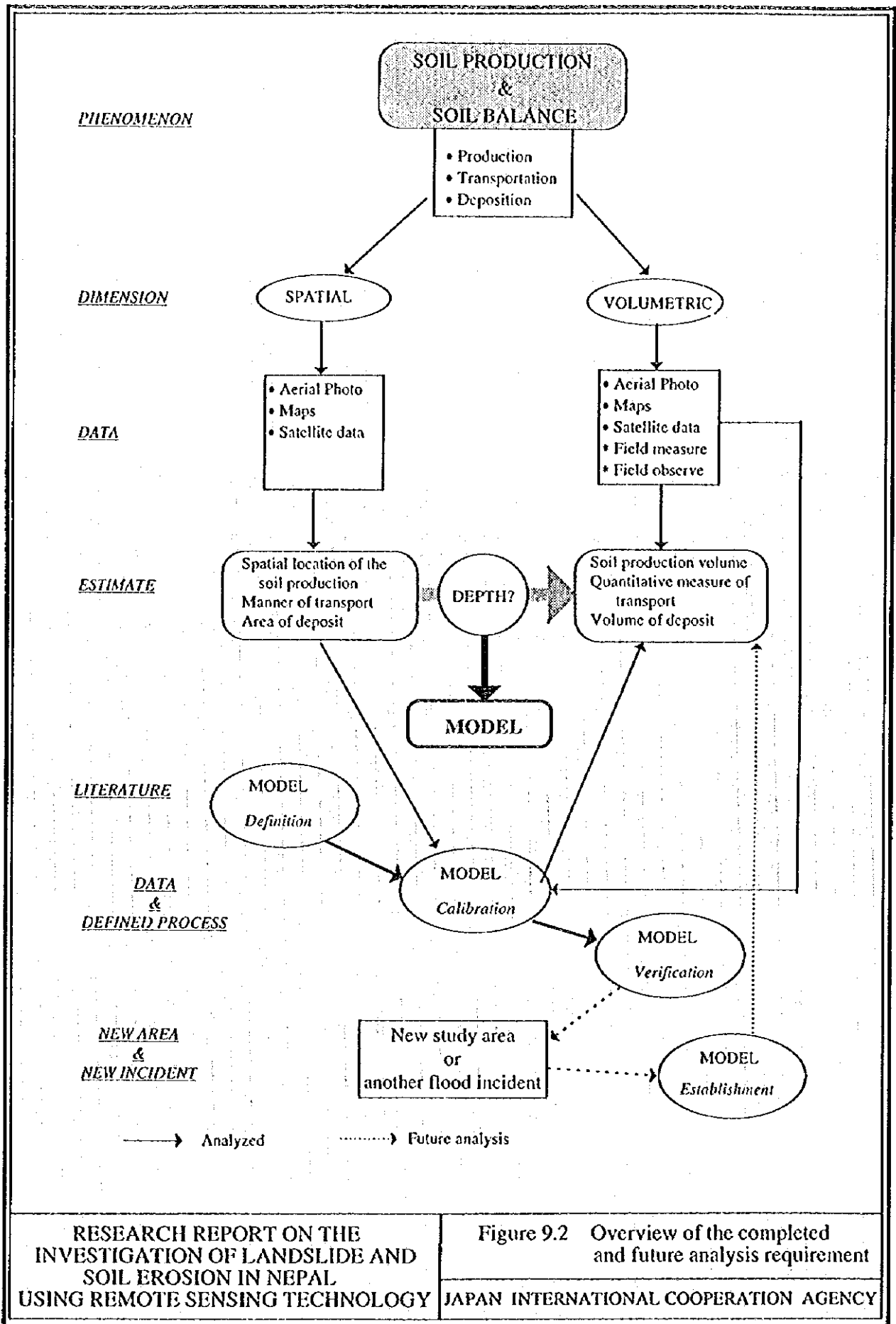
Figure 9.2   Overview of the completed and future analysis requirement

RESEARCH REPORT ON THE INVESTIGATION OF LANDSLIDE AND SOIL EROSION IN NEPAL USING REMOTE SENSING TECHNOLOGY	Figure 9.2 Overview of the completed and future analysis requirement
	JAPAN INTERNATIONAL COOPERATION AGENCY

- The riverbed changes in the upper watershed was estimated as 0.14 sq.km per year. This estimation can satisfactorily be used for a time span of more than 4 years.

- It was found that NDVI was related to land degradation. Also, the NDVI estimation showed that the forest cover is degrading in this area gradually for the last 22 years for which the analysis was carried out.

- Satellite data can be used in identifying newly deposited areas and old river beds in the floodplain.

- Monitoring the river channel changes in the flood plain can satisfactorily be carried out using remote sensing data. This may facilitate the mitigation of hazardous areas during a flood event if supported by few field investigations in the high riverbed accumulation areas.

- It is observed that two dates satellite data, wet and dry seasons are required to accurate land cover mapping in this watershed due to high heterogeneity in the land use.

- The planform changes of deposition in the compared watershed is similar to Ratu watershed, hence the use of satellite data in planform change assessment in the Siwalik area is justified.

On these observations it can be said that the satellite data can satisfactorily be used to gather information pertaining to soil erosion such as, planform changes, monitoring of river channels, and the state of forest degradation in Siwalik area.

Results of Volumetric Changes and Monitoring

- Soil erosion process during a flood event of the Ratu watershed was clearly identified and established using the field observations. It was found that the soil erosion during a flood event is highly related to topographical and geological condition of the sub-streams. It was estimated an amount of 2 million m³ of soil has been produced during the 1993 flood event.

- Average annual soil production under a normal condition was estimated by a model that is based on satellite data derived NDVI, and surface slope. The calibration of this model was carried out using average denudation rates published for Eastern Nepal. Further, time series analysis of average annual soil production showed that the average denudation rate of the Ratu watershed is increasing, and the 1993 average value is 3.9 mm/year.

- Estimation of soil production under 1993 flood event was carried out modifying the model by integrating *flood event erosion index* which is depend on sub-stream density in a watershed. The estimated volume using this model was 2 million m^3 for a flood event.

- Prior establishment of flood event index using GIS technology, and acquiring a remote sensing data before a rainy season facilitate the estimation of soil production for a watershed in Siwalik during a flood event with an order of 1993 floods.

On these observation it could be said that the volumetric estimation of soil production using remote sensing can only be materialized if integration of GIS is considered.

The developed model for annual soil production is based on empirical values of denudation. This model has been tested for its accuracy in Japan, but it is advisable to evaluate the results in a regulated watershed that has reliable denudation rates for verification.

The modified model for flood event soil production assessment was calibrated using field observed production volume of 1993 flood event. This model has to be verified in some other watershed, or during a different flood event in for verification and for any modification in view of establishing as a flood event soil erosion model of Siwalik area.

9.2 Configuration of a Data Analysis System for DPTC

It was considered to transfer the know how of the present model and remote sensing and GIS technology to the counterparts in Water Induced Disaster Prevention Center (DPTC) of Nepal. DPTC is established in Nepal with the collaboration of HMG/N and JICA to transfer appropriate technology to local engineers in water induced disaster prevention. This would involve damage assessment, monitoring, and forecasting as these fields can not be ignored when carrying out prevention action. A counter measure could be a civil engineering work, bio-engineering method or introduction of some social and cultural changes, but selecting the best suitable counter measure should consider the spatial characteristics of the problem in hand. In this sense, properly maintained information system could facilitate selecting the best methodology, comprehensively. This aspect of the disaster prevention program could be considered as monitoring. Another branch of the disaster prevention action could be the giving out accurate and timely information about a disaster before that could affect the society in danger. This is referred to as forecasting, and requisite knowledge of historical incidents and the spatial and temporal characteristic of the area of interest. Lack of information makes a task difficult, specially in disaster proven country like Nepal where most of the construction projects might have carried out without ample information.

Necessity to have a spatial information system that can handle data sources from maps, images, tables and field investigation with respect to water induced disasters within the DPTC is unquestionable. To achieve this, one should clearly defined the service area of DPTC and the scale of the problems that the center is willing to address.

The most common water induced disasters in Nepal are floods and landslides. These incidents can be approached or discussed in two different level; *event specific* and *cause specific*. If a flood event is taken as event specific it is only required to consider the spatial location of the interested river and its

surrounding extending for few meters. If the flood is discussed as cause specific level, it is required to extend the discussion from river to its watershed. As it is known a flood will not occur only from a degraded watershed without considerable rainfall the discussion may have to be further extended from the watershed level to regional or country level. This shows that prevention in engineering aspect needs only site specific information, bio-engineering implementation may required to consider in a watershed scale and leading to regional scale for better assessment.

The preceding discussion shows that an ideal water induced disaster prevention database should include information from site specific to regional scale. Then the question that should be answered is, whether there a necessity to create a database from scratch to use in disaster prevention, monitoring and forecasting works at the DPTC. Incidentally, it was observed during the GIS agency survey that some are progressing towards country level database which may be fully utilized some where within this year. Specifically, ICIMOD has been completed a small scale database for whole Nepal including topography, landuse, physiography, socio-economic data obtained from 1:250,000 maps. Tribhuvan University is moving towards to establish a more detailed database with the collaboration of ICIMOD using one inch topographical maps. Their target is to complete an elevation database based on one inch maps within few months time. FRIS is already finished a forest resources mapping program for the whole country using satellite data of 1990 and 91 at Forest Survey and Statistics Division. It could be considered these data may be freely available once they have become operational as the DPTC is non-profitable organization. This would let a good starting point to start GIS and remote sensing activities in the field of water induced disaster at DPTC.

It was observed during the visit to different agencies the coordination among agencies is poor except for personal level. There is a need to from a country level steering committee for coordination and to avoid repetition in data creation. This may not be possible to achieve at present due to lack of experience of the usage of these technologies and hardly any projects that

have really explored the potential of remote sensing and GIS technologies here in Nepal. In this sense, it is highly recommendable to start a GIS and remote sensing system at DPTC with a low profile, educating and training staff being a user of already developed databases to explore the potential of these technologies in fulfilling the center goals.

With the understanding of the goals of the DPTC, a system recommendation for the center was considered. Properly organized remote sensing and GIS system should comprise with following components;

     1. Appropriate hardware and software
     2. Skilled personnel to operate and carry out analysis
     3. Maintenance system

It is recommendable to initiate and implement a system at DPTC in three phases rather than setting up a system for multi purpose studies considering the lack of skilled staff and the cost of initial system installation. Also, consideration has to be made to acquire permanent staff for the system as the training of personnel involves time and money. Temporary staff acquired from interested agencies or departments have to return back to original posts if they are asked to. Therefore, it is advisable to avoid staff in lease basis. Maintenance of the system is very important as the hardware could break down or software could be obsolete after some time. Further, for monitoring the area of interest continues supply of remote sensing data, at least one set for year has to be incorporated to the database for timely and up to date information.

Phase I

This is the initial stage, and should addressed only the field of GIS which can be easily mastered and practiced. In selecting software, consideration has to be given to the software used by other agencies. It is recommend to have a

system configuration as shown in Figure 9.3. This configuration helps to share arc/info data files through DAT or 1/4 tapes. Also, this system serves for in house data creation where maps can be digitized on PC either using arc/info or any other software that could create arc/info compatible data files (AutoCad). Two hardware set up gives the opportunity to do the data creation and analysis at the same time.

It is advisable to recruit three members at this phase, one for digitizing and other two with engineering knowledge in the disaster prevention. Parallel to system installation, the staff should be educated in data creation as the first step. This level of training may be given at TU or ICIMOD. When the staff acquired the basic knowledge the engineers could undergo training on analysis. This could be carried out by inviting experts from other agencies in here or from abroad. The first phase could run for one year. In the latter part of this phase, one engineer should undergo some training in remote sensing. Local training center for this could be the FSSD, where he can be exposed to data and to popular software. Computer systems and external peripherals should
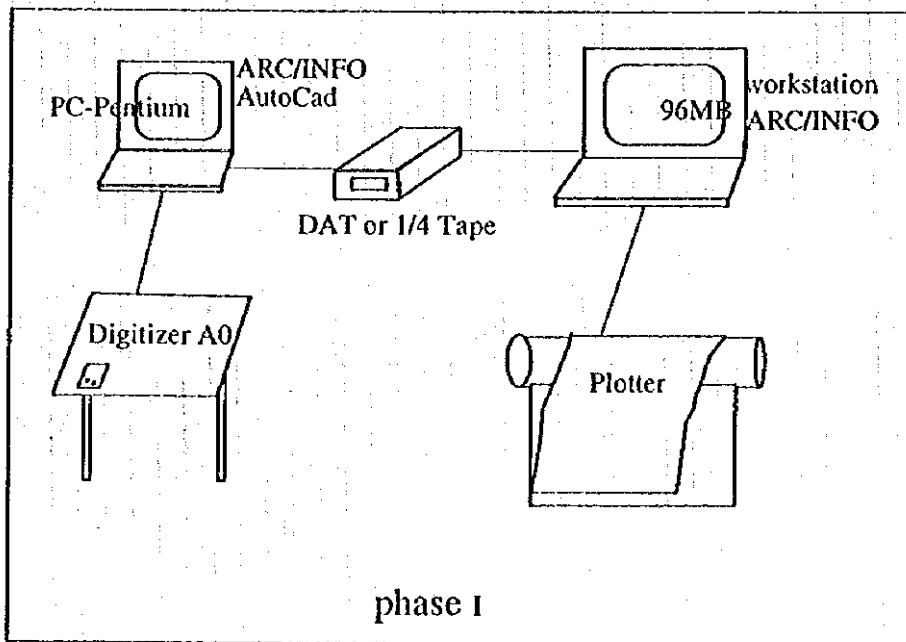

Figure 9.3 System configuration for phase I

Unlike GIS, remote sensing operation needs special knowledge of different sensors, different data formats supplied by receiving centers, correction methods, classification methods, integration with GIS etc. The engineer who was exposed to remote sensing at phase one should further undergo short training while working on a specific task to acquire more knowledge on this bring on to a network environment to avoid difficulties in data transfer and analysis in later stages.

Phase II

Finishing the first phase, the staff at the center could have acquired basic knowledge of GIS and remote sensing and may be in a position to create GIS data for needs of the center. In this stage the capability of GIS should be increased in the field of application. This can be carried out by exposing the GIS engineer to experts from JICA or creating collaboration works with other agencies.
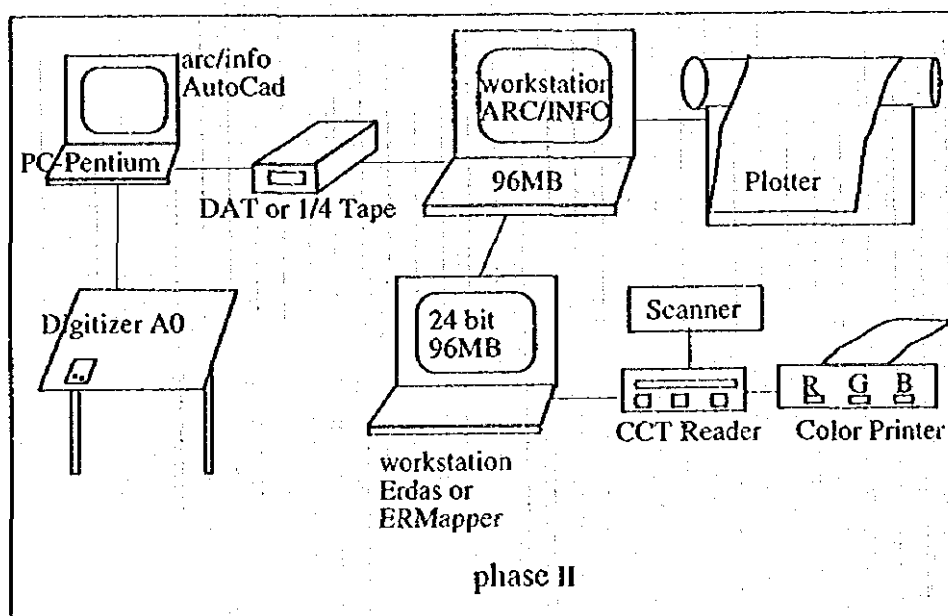

Figure 9.4 System configuration for phase II

In this stage a remote sensing system will be added to the present configuration making the center a fully equipped remote sensing and GIS to

work as an independent body. A system as in Figure 9.4 can be considered at this stage.

field. Consideration can be given to send the person abroad or invite specialists for short period to work together. This phase may run for one year adding one more year to the center. In these two stages the analysis could be carried out to characterize water induced phenomena, damage assessment and hazard mapping. Note that there should be sufficient disk space for remote sensing analysis as the data itself occupies considerable amount of memory, (Landsat full scene is about 250 MB).
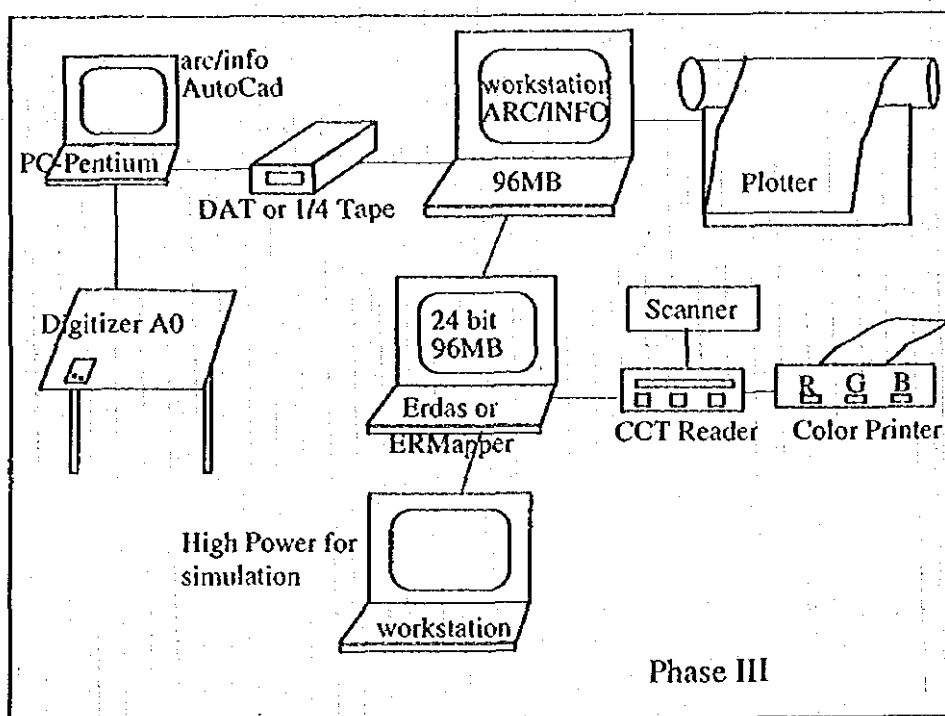
Phase III

Figure 9.5 System configuration for phase III

This phase is considered as more advanced step of the computer assisted planning, monitoring and forecasting of water induced disasters in Nepal. It is suitable to include the forecasting technology by simulation of natural hazards

for inform the society in advance. The system should be upgraded with additional computer, preferably a high performance workstation for CPU intensive simulation. Simulation models could be developed in house or supported by foreign experts. In this phase, Figure 9.5, the system enable to integrate simulation results with GIS database for forecasting of natural hazards, identifying vulnerable areas and better ways to avoid large scale loss of life and property. Training of personnel in forecasting could involve expertise from different fields of applications; soil erosion, geomorphology, geology, mathematics, fluid dynamics, hydraulics etc. and may not be able to accomplish within a short time. The required technology have to be transferred from sponsor organizations, at least at the beginning.

REFERENCES

Burrough, P.A.: *Principles of Geographical Information Systems for Land Resources Assessment*, 1986, Clarendon Press Oxford

Honada, K, Murai, S., and Shibasaki, R.: *Prediction of vegetation restoration by erosion control works in Asio copper mine Japan*, 13th IGRSS, 1993

ICIMOD: *The Role of Extreme Weather Events, Mass movements, and Land Use Changes in Increasing Natural Hazards*, 1993

Ives, J. D. and Messerli, B.; *The Himalayan Dilemma*, Routledge London and New York, 1989

Ives, J.D.: *The theory of Himalayan environmental degradation: Its validity and application challenged by recent research*, Mountain Research and Development, Vol. 7, No. 3, 1987

Iwata, N.: *Rising Himalaya*, Chikuji Shokan, Tokyo, 1988 (In Japanese)

Matsuda, T.: *Magnitude of tectonics movement and its frequency*, Geography, 4, 151-165, 1983 (In Japanese)

Sharma, K. C.: *Natural Resources in Nepal*, 1978

Sharma, K. C.: *Natural Hazards and Man made Impact in Nepal Himalaya*, 1988

Sharma, K.C.: *Some Symptoms of Environmental Degradation in Nepal (1950-1994)*, 1995, Printing Support Pvt. Ltd. Katmandu

Summerfield, M. A.: *Global Geomorphology, Longman Scientific & Technical*, 1991

Yamamoto, K.: *Theory of Channel Form*, Public Works Research Institute Papers, Vol. 2662, 37-50, 1988